İSTANBUL TECHNICAL UNIVERSITY ★ GRADUATE SCHOOL OF SCIENCE ENGINEERING AND TECHNOLOGY

PARAMETER OPTIMIZATION FOR z-FACTOR CORRELATIONS TO PREDICT JOULE-THOMSON INVERSION CURVE

M.Sc. THESIS

Muhammed Said ERGÜL

Department of Petroleum and Natural Gas Engineering

Petroleum and Natural Gas Engineering Program

DECEMBER 2018

İSTANBUL TECHNICAL UNIVERSITY ★ GRADUATE SCHOOL OF SCIENCE ENGINEERING AND TECHNOLOGY

PARAMETER OPTIMIZATION FOR z-FACTOR CORRELATIONS TO PREDICT JOULE-THOMSON INVERSION CURVE

M.Sc. THESIS

Muhammed Said ERGÜL
(505151524)

Department of Petroleum and Natural Gas Engineering

Petroleum and Natural Gas Engineering Program

Thesis Advisor: Asst. Prof. Dr. Şenol YAMANLAR

DECEMBER 2018

İSTANBUL TEKNİK ÜNİVERSİTESİ ★ FEN BİLİMLERİ ENSTİTÜSÜ

JOULE THOMSON TERSİNME EĞRİSİNİN BULUNMASINDA z-FAKTÖRÜ KORELASYONLARI İÇİN PARAMETRE OPTİMİZASYONU

YÜKSEK LİSANS TEZİ

Muhammed Said ERGÜL
(505151524)

Petrol ve Doğal Gaz Mühendisliği Anabilim Dalı

Petrol ve Doğal Gaz Mühendisliği Programı

Tez Danışmanı: Dr. Öğr. Üyesi Şenol YAMANLAR

ARALIK 2018

Muhammed Said ERGÜL, an M.Sc. student of ITU Graduate School of Petroleum Engineering student ID 505151524, successfully defended the thesis entitled "PARAMETER OPTIMIZATION FOR z-FACTOR CORRELATIONS TO PREDICT JOULE-THOMSON INVERSION CURVE", which he prepared after fulfilling the requirements specified in the associated legislations, before the jury whose signatures are below.

Thesis Advisor: **Asst. Prof. Dr. Şenol YAMANLAR**
İstanbul Technical University

Jury Members: **Assoc. Prof. Dr. Gürşat ALTUN**
İstanbul Technical University

Asst. Prof. Dr. Ali ETTEHADİ
İzmir Katip Çelebi University

Date of Submission : 16 November 2018
Date of Defense : 14 December 2018

To my family

FOREWORD

I would like to thank my thesis advisor Dr. Şenol YAMANLAR to support and guidance on my thesis. Additionally, I would like to thank my family and my friends for their support.

December 2018

Muhammed Said ERGÜL
(Petroleum and Natural Gas Engineer)

TABLE OF CONTENTS

Page

ABBREVIATIONS

JTIC	**:** Joule-Thomson inversion curve
DAK	**:** Dranchuk-Abou Kassem
DPR	**:** Dranchuk-Purvis-Robinson
HY	**:** Hall-Yarborough
SSE	**:** Sum of squares error

SYMBOLS

μ_{JT}	:	Joule-Thomson coefficient
T_c	:	Critical temperature, K or R
P_c	:	Critical pressure, psia or bar
T_{pr}	:	Pseudo-reduced temperature
P_{pr}	:	Pseudo-reduced pressure
H	:	Enthalpy, kJ/kg or Btu/lbm
V	:	Molar volume, ft^3/lb-mol or m^3/mole
S	:	Entropy, kJ/°K or kcal/°R
C_p	:	Heat capacity, J/g °K or Btu/lb °R
T	:	System temperature, K or R
P	:	System pressure, psia or bar
z	:	Gas compressibility factor
R	:	Universal gas constant, ft^3 psi/R lb-mol or m^3bar/K gr-mol

Subscripts

pr	:	Pseudo-reduced condition
c	:	Critical condition

LIST OF TABLES

Page

LIST OF FIGURES

Page

PARAMETER OPTIMIZATION FOR z-FACTOR CORRELATIONS TO PREDICT JOULE-THOMSON INVERSION CURVE

SUMMARY

When a real gas undergoes a volumetric process, a temperature change is usually observed. Temperature change is experienced during production at the perforations, throughout surface and subsurface chokes, at the surface where heavier hydrocarbons are removed at the processing facilities and compression and liquefaction of natural gas. Temperature change accompanying volumetric change is known as Joule-Thomson effect. The sign and magnitude of the temperature change may be determined by using Joule-Thomson coefficient.

If Joule-Thomson coefficient is positive, then the gas temperature decreases as a result of expansion. Under the condition where the coefficient is negative, expansion process increases the gas temperature. If Joule-Thomson coefficient is identically zero, no temperature change will be observed as a result of volume change. Projection of the pressure-temperature pairs at which Joule-Thomson coefficient becomes zero creates an envelop on the P-T plane. This envelop is known as Joule-Thomson inversion curve. The inversion curve separates the P-T plane into two regions where the temperature changes have opposite signs. All gases have different inversion conditions.

Measurement of inversion condition for gases requires precisely controlled experimental conditions. As a result of experienced difficulties in the experimental setups, the inversion data is limited in the literature. In lack of sufficient experimental data, some correlations, equation based prediction methods and molecular simulation techniques are all used to compute the inversion characteristics of the different gases. None of these methods are able to predict the inversion conditions accurately.

The aim of this study is to search the applicability of several z-factor correlations extensively used in petroleum and natural gas engineering in prediction of Joule-Thomson inversion curve. Adjustable parameters of the correlations would be optimized to improve the accuracy of the inversion curve computations. Since these equations are readily programmable, they will be valuable tool in engineering calculations.

JOULE-THOMSON TERSİNME EĞRİSİNİN BULUNMASINDA z-FAKTÖRÜ KORELASYONLARI İÇİN PARAMETRE OPTİMİZASYONU

ÖZET

Joule-Thomson etkisi gazların sabit entalpi şartları altında hacimsel değişime maruz kalması sonucunda ortaya çıkar ve bu olay çoğunlukla gazlarda sıcaklık değişimiyle sonuçlanır.

Joule-Thomson etkisi ilk olarak James Joule ve William Thomson tarafından gerçekleştirilen bir deneyde keşfedilmiştir. Bu deneyde gazlar sabit entalpi koşulları altında basınç değişimine maruz bırakılmış ve hacim değişimine uğrayan gazların sıcaklıklarında değişim gözlenmiştir. Deneyler sonucunda ilk durumdaki sıcaklık ve basınç değerlerine bağlı olarak gazların sıcaklığındaki değişimin artan veya azalan doğrultuda olabileceği fark edilmiştir.

Bu artış veya azalışın doğrultusu Joule-Thomson katsayısıyla modellenir. Eğer Joule-Thomson katsayısı sıfırdan büyükse genleşen gaz soğur ve eşdeğer olarak hacmi düşürülen gaz ısınır. Katsayının sıfırdan küçük olması durumda ise genleşen gaz ısınır ve eşdeğer olarak sıkışan gaz soğur. Joule-Thomson katsayısının sıfıra eşit olduğu durumlarda ise gazların sıcaklığında bir değişim gözlenmez.

Joule-Thomson katsayısının sıfıra eşit olduğu basınç-sıcaklık ikililerinin basınç-sıcaklık düzleminde izdüşümü bir eğri oluşturur. Bu eğriye Joule-Thomson tersinme eğrisi adı verilir. Bu eğri genleşme ile oluşan artış veya azalış yönündeki sıcaklık değişim bölgelerini birbirinden ayırır. Eğrinin içinde kalan bölgede genleşme sonucunda soğuma görülürken, eğrinin dışında kalan bölgede genleşme ile ısınma görülür. Farklı gazlar için eğrinin şeklinde benzerlik olsa da farklı gazlar farklı tersinme değerlerine sahiptirler.

Petrol ve Doğal Gaz mühendisliği alanının birçok uygulamasında sıcaklık ve basıncın doğru olarak modellenmesi ancak doğru Joule-Thomson etkisinin bilinmesiyle mümkün olmaktadır. Özellikle doğal gazın kuyu içerisine perforasyonlardan geçerek akışı sırasında, üretim borularıyla yüzeye taşınmasında ve yüzeyde genleştirilerek içerisindeki ağır hidrokarbonlardan uzaklaştırılması sırasında gaz sıcaklığında değişimler görülür. Ayrıca Joule-Thomson etkisinin doğru olarak tahmin edilmesi kuyu testlerinin sonuçlarının yorumlanmasında da önemlidir.

Gazların tersinme noktalarını belirlemek için çok hassas sıcaklık ölçümlerine ve basınç kontrol mekanizmalarına ihtiyaç vardır. Deneysel düzenekte karşılaşılan zorluklardan dolayı literatürde deneysel olarak belirlenmiş tersinme basınç ve sıcaklık verisi oldukça kısıtlıdır. Bu alandaki eksikliğin giderilmesi için bazı korelasyonlar, durum denklemi yaklaşımları ve moleküler simülasyon yöntemleri ile tersinme eğrisi verileri elde edilmeye çalışılmıştır. Denenen yöntemler ile elde edilen tersinme eğrileri özellikle yüksek sıcaklık ve yüksek basınç bölgelerinde (üst tersinme eğrisi) hatalı sonuçlar vermekte ve değerler kullanılan yaklaşıma bağlı olmaktadır.

Bu çalışmanın amacı petrol ve doğal gaz mühendisliğinde yaygın olarak kullanılan z-faktörü korelasyonlarının (gaz sıkıştırılabilirlik faktörü ya da gaz sapma faktörü olarak da isimlendirilir) Joule-Thomson tersinme eğrilerinin hesaplanması amacıyla uygulanabilirliklerinin araştırılmasıdır. Ayrıca kullanılan iki parametreli indirgenmiş durumlar yasasına uyan bu korelasyonların katsayılarının optimize edilerek tersinme eğrilerinin daha duyarlı olarak hesaplanabilirliğini göstermektir.

Bu amaç kapsamında kullanılan z-faktörü korelasyonları, Dranchuk-Abou Kassem korelasyonu, Hall-Yarborough korelasyonu ve Dranchuk-Purvis-Robinson korelasyonudur. Her üç korelasyonda iki parametreli eşdeğer durumlar yasası temellidir. Kullanılan korelasyonların deneysel olarak elde edilen z-faktörü değerlerinin doğrusal olmayan regresyon analizi yöntemiyle parametreleri elde edilmiştir. Ayrıca bu korelasyonlar ayarlanabilir katsayılara sahip olduklarından, deneysel verilere göre yapılacak parametre tahmini ile mevcut formları korunarak yeni parametreler geliştirilebilecektir.

Bu çalışma kapsamında, öncelikle Joule-Thomson katsayısı gaz sıkıştırılabilirlik faktörü değerinin sabit basınçta sıcaklığa göre değişimi (sabit basınçta z faktörü değerinin sıcaklığa göre türevi), evrensel gaz katsayısı, ısı kapasitesi, basınç ve sıcaklık parametrelerine bağlı olarak matematiksel olarak bir denklem formunda tanımlanmıştır. Bu denklemde türev terimi hariç diğer tüm terimler pozitif değerler alabileceğinden Joule-Thomson katsayısının işareti sadece gaz sıkıştırılabilirlik faktörünün türevi tarafından kontrol edilir. Tersinme eğrisinin hesaplanmasında denklemin sağ tarafının sıfır değerini alması ile sıcaklığın, basıncın ve ısı kapasitesinin etkileri de ortadan kalkar ve yalnızca z faktörünün sabit basınçta sıcaklığa bağlı olan değişiminin sıfıra eşit olduğu noktanın bulunması yeterlidir.

Yukarıda adları geçen korelasyonlar indirgenmiş basınç ve sıcaklığın fonksiyonu olduğundan, Joule-Thomson katsayısı denkleminin indirgenmiş büyüklükler cinsinden yeniden yazılması gerekir. Bu ifadenin geliştirilmesi ile z-faktörünün indirgenmiş sıcaklığa göre türevi Dranchuk-Abou Kassem, Hall-Yarborough ve Dranchuk-Purvis-Robinson korelasyonları kullanılarak bulunmuştur. Joule-Thomson tersinme eğrisi z faktörünün sabit indirgenmiş basınçta, indirgenmiş sıcaklığa göre türevinin sıfır olduğu noktalar olarak hesaplanmıştır. Oluşturulan tersinme eğrileri literatürdeki metan deneysel verileri ve yine referans olarak kabul edilen REFPROP (referans termofiziksel özellikler programı) uygulamasından elde edilen metan tersinme değerleri ile karşılaştırılmıştır.

Karşılaştırılma sonucunda Dranchuk-Abou Kassem korelasyonu alt tersinme eğrisinin tahmininde deneysel verilerle uyum gösterirken, maksimum tersinme basıncı noktası civarında deneysel verilerden farklılık göstermiştir. Üst tersinme eğrisinin tahmininde ise korelasyon aynı başarıyı gösterememektedir. Benzer olarak Hall-Yarborough ve Dranchuk-Purvis-Robinson korelasyonları da alt tersinme eğrisinde deneysel değerlerle benzerlik gösterirken maksimum tersinme basıncı noktası ve üst tersinme eğrisinde iyi sonuçlar verememiştir. Dranchuk-Purvis-Robinson korelasyonu fonksiyonel form olarak Dranchuk-Abu Kassem korelasyonunun öncüsü olduğundan dolayı, sonuçları da benzerlikler göstermektedir. Hall-Yarborough korelasyonu ise fonksiyonel olarak değişik bir forma sahiptir. Bundan dolayı maksimum indirgenmiş basınç civarında farklılaşmaya başlamakla birlikte, yüksek indirgenmiş basınçlarda üst tersinme eğrisini orijinal katsayılarla tahmin etmede daha başarılıdır.

Tez çalışmasının amacı doğrultusunda z-faktörü korelasyonlarının tersinme eğrisinin her bölgesini doğru bir şekilde tahmin edebilmesi için Dranchuk- Abou Kassem ve

Hall-Yarborough korelasyonlarının katsayıları, literatürdeki deneysel veriler ve REFPROP verileri kullanılarak optimize edilmiştir. Yapılan optimizasyon işlemiyle Hall-Yarborough korelasyonu referans değerlerle tam uyum gösterirken, Dranchuk-Abou Kassem denklemi çok az miktarda da olsa referans değerlerden sapma göstermiştir. Buna ek olarak Dranchuk-Abou Kassem korelasyonunun daha doğru sonuçlar verebilmesi için optimizasyon işlemi iki parçada yapılmıştır. Bunun için referans olarak kullanılan değerler alt ve üst tersinme eğrilerini temsil edecek şekilde iki parçaya bölünmüş ve her iki veri setinde de ortak noktalar regresyona dahil edilmiştir. Her bir veri seti için Dranchuk-Abou Kassem parametreleri yeniden bulunmuştur. Bu işlemle iki farklı parametre seti oluşturulmuş ve bu parametre setinden bir tanesi alt tersinme eğrisini diğeri üst tersinme eğrisinin tahmin edilmesinde kullanılmıştır. Tahmin edilen sonuçlar referans sonuçlarla tüm bölgelerde tam olarak uyum göstermiştir.

Bu çalışma kapsamında ayrıca, korelasyonlarla elde edilen tersinme değerlerinin hata analizleri yapılmış ve parametreleri iki parça halinde optimize edilmiş Dranchuk-Abou Kassem korelasyonu tersinme eğrilerinin tahmini için en iyi alternatif olduğu saptanmıştır.

1. INTRODUCTION

All real gases undergo temperature changes when their volume is changed. Temperature of natural gas also changes during production at the perforations, inside the tubing, through the surface chokes and at the surface where heavier hydrocarbons are removed at the processing facilities. The change of the gas temperature at the different parts of the production system depends on the prevailing pressure and temperature conditions. Depending on the initial pressure and temperature condition of gas, temperature change could be in either increasing or decreasing direction. This phenomenon is known as Joule-Thomson effect in thermodynamics.

Proper prediction of Joule-Thomson effect is needed in petroleum industiries especially in gas reservoirs applications. Accurate knowledge of temperature and pressure conditions in production string is critical for many applications.The Joule-Thomson effect should be properly included in numerical simulation equations in order to get correct results in gas flow calculation.

In petroleum and natural gas reservoir engineering applications, reservoir fluid temperature will be decreased by expansion in general. Nevertheless, temperature increases of a few degress are possible in high pressure-high temperature (HPHT) reservoirs. Such bottomhole temperature increases around the perforations are reported by Jones [1] and by Baker and Price [2].

The importance of Joule-Thomson effect has been subject to lots of studies some of them is given below:

Jamaloei and Asghari [3] presented a study about Joule-Thomson effect in well testing, production testing and monitoring. According to them Joule-Thomson cooling is one of the important dynamic parameters lead to diffences between flowing bottomhole temperature and static formation temperature at that depth. They also mentioned that hydrocarbons flowing from formation to the well experince a pressure drop that causes temperature changes in the fluid because of the Joule-Thomson effect.

Jamolei and Asghari [4] present another study about the Joule-Thomson effect as a second part of the previous study. In the second part they mentioned Joule-Thomson effect on carbon dioxide injection into depleted gas reservoirs, prediction of wellbore temperature profiles, and the impact of thermal stress on the wellbore stability.

Another study about Joule-Thomson effect belongs to Pakulski [5]. In his study, during flow-back operations and production in deeper water, he showed the cases that hydrate formation observed mostly due to Joule-Thomson effect.

Batesole and Wilkes [6] have mentioned Joule-Thomson effect in underground gas storage. They stated that the Joule-Thomson effect is usually the dominant factor in determining the change in gas temperature for underground storage reservoirs. It is most notable near the wellbore where most of the pressure drop takes place, and is therefore, a greatly contributing factor to hydrate formation.

Oldenburg [7] targeted the importance of Joule-Thomson cooling effect during carbon dioxide injection into depleted gas reservoirs. He stated that formation permeability and so, injectivity could be decreased by formation of hydrates when the Joule-Thomson cooling effect was large.

Steffensen and Smith [8] were the pioneer who explained the influence of Joule-Thomson effect in the interpretation of temperature logs. Joule-Thomson heating of water and cooling of gas can have notable amount of influence on temperatures because of pressure drop during flow around the production-injection wells.

App [9] stated that the importance of Joule-Thomson effect could not be disregarded in high-pressure low permeability reservoirs. The high drawdown in such reservoirs could increase wellbore temperatures due to Joule-Thomson expansion of reservoir fluids.

2. LITERATURE REVIEW

The prediction of inversion curve has been a subject to many studies in the literature. There are studies in the literature about direct measurement of Joule-Thomson inversion data as well. The early studies of the Joule-Thomson effect and inversion curve are generally experimental works.

As one of the early studies, Roebuck and Osterberg [10-12] measured the Joule-Thomson coefficient of helium and described their methodology and apparatus used in work. In addition, they extended their study for argon and nitrogen using the same apparatus. Using the same experimental apparatus they also provided the Joule-Thomson inversion curve data.

Another pioneer study presented by Budenholzer et al. [13]. They determined the Joule-Thomson coefficient of methane at a temperature range of 294.26 °K to 377.5944 °K and for pressure range of atmospheric pressure to 10.3421 MPa.

Gunn et al. [14] stated that directly determining the values of Joule-Thomson coefficient was difficult and unreliable in the vicinity of inversion point. For this reason, they generate a correlation that is function of reduced parameters for nearly spherical molecules. For this purpose, Joule-Thomson inversion data including argon, methane, ethane, carbon monoxide were used from various literature studies.

According to Miller's [15] study, Joule-Thomson inversion data can be determined for all gases effectively by applying corresponding states principle with the exception of hydrogen (H_2) and helium (He). He generated an empirical correlation from the existing Joule-Thomson inversion data, moreover the shape of inversion curve, $T_{r,max}$ (reduced maximum inversion temperature) and $T_{r,min}$ (extrapolated minimum reduced inversion temperature) were discussed. He found that among the other equations of state (EOS), inversion curve Redlich-Kwong EOS was the best equation in predicting the inversion curve. Miller also stated that prediction of the inversion curve is a real test for predictive ability of an EOS.

In Dilay and Heldemann's [16] study, four equation of states Soave-Redlich-Kwong (SRK), Peng-Robinson (PR), perturbed hard-chain (PC) and Lee-Kesler (LK) were studied for their capacity to predict the Joule-Thomson inversion curve. All of them were able to predict lower branch of the inversion curve, but none of the equations produced adequate results at the upper part of curve. Lee-Kessler equation produced the most precise prediction data among the others. The authors also mentioned that calculated low-temperature branch of inversion curve was not sensitive to the EOS parameters. However, the maximum point of inversion curve and high-temperature branch show great deviations increasing with the acentricity.

Colazo et al. [17] were compared the seven cubic equation of state to predict the inversion curve for simple fluids. The results compared with empirical correlation presented by Gunn et al. This comparison indicated that the predicted maximum inversion pressure directly depends on the difference between EOS and real fluid critical compressibility factors. Among the seven equations, original Redlich-Kwong (RK) EOS, the Martin (1979) Clasius type EOS and Trebble -Bishnoi EOS were found to be the most suitable ones.

Maghari and Matin [18] studied the ability of five van der Walls type EOS to predict the Joule-Thomson inversion curve. Adachi-Lu-Suqie, Kubic-Matin, Twu-Coon-Cunnigham and Deiters predict lower part of Joule-Thomson inversion curve adequately except Yu-Lu equation of state. According to authors, usually high temperature part and maximum point of inversion curve are verified to be sensitive to the used EOS. The result of the study shows that Deiters EOS supplied the most correct prediction in the sensitive part.

Darwish and Al-Muhtaseb [19] compared four different EOS' for the prediction of inversion curve and spinodal curve loci of methane. They discussed the difference of prediction and experimental data with using Gunn et al. correlation. They found that Trebble-Bishnoi equation were reliable at reduced temperatures of below 2.3. Redlich-Kwong and modified Peng-Robinson equations were good below reduced pressure of 9.5 and 10 respectively.

Colina and Olivera-Fuentes [20] developed new version of van der Walls, Redlich-Kwong and Peng-Robinson EOS' using experimental inversion data of air. These modified equations produced better results than more complex, multi-parameter noncubic equations of state.

Castillo et al. [21] used Lee-Kesler and Boublik-Alder-Chen-Kreglewski equation of states to predict Joule-Thomson inversion curve for non-simple fluids and they generated new correlations depend on these EOS' as a basis. They suggested that predictions were fairly reliable and these data can be used in place of experimental values.

Matin and Haghighi [22] used some equations of states that include two, three or four parameter cubic EOS for testing adequacy of prediction of Joule-Thomson inversion curve. These EOS' were modified Patel-Teja (MPT), modified Peng-Robinson (MPR) by Melhem-Saini-Goodwin, Iwai-Margerum-Lu (IML), modified Redlich-Kwong (MRK) by Souahi-Albane-Kies-Chitoreu and Trebble-Bishnoi (TB). All of the equations tested in their study gave agreeable results for the lower part of the inversion curve. In the maximum point of the curve and above, TB equation showed relatively sufficient match with experimental data and Gunn, Chuech and Prausnitz correlations.

Colina and Müller [23] used isobaric-isothermal Monte Carlo molecular simulation to predict the Joule-Thomson inversion curve for Lennard-Jones fluid. They also mentioned that molecular simulations may be used to predict thermophysical properties at experimentally inaccessible conditions.

In Chacin et al. [24] study, the Joule-Thomson inversion curve for carbon dioxide was predicted by using molecular simulation technique. The Lennard-Jones model was employed for modeling the fluid-fluid interactions. The simulation results were compared with experimental data. The predicted results were quantitatively agreeable to the experimental data.

In Collina et al. [25] study, prediction of Joule-Thomson inversion curve for CO_2 and n-alkane series was done by using molecular based the Soft SAFT equation of state. Comparison with the experimental and correlative data showed good agreement. There was a strong dependency on the set of molecular parameters used in the simulation runs especially near the maximum point of the inversion curve and in the high temperature region. Soft-SAFT equation enable to predict inversion curve for a condition that reduced pressure values up to 40 and reduced temperature values up to almost 5.

Haghighi et al. [26] compared five EOS' in predicting the inversion curve. Among those, modified SRK equation of state by Mathias and Copeman and Harmens-Knapp

equations produced good predictions in the low temperature region. The predictions of modified Peng-Robinson EOS by Ruzy and Vdw11 equations were found to be inadequate.

Vrabec et al. [27] presented the molecular simulation results of the Joule-Thomson inversion curves for 15 pure fluids and air as a mixture and compared these results with a reference EOS. The comparison gives excellent matches for full range of inversion curve. They claimed that molecular models can be employed reliably for the simulation of molecular scale phenomena.

Bessieres et al. [28] used pressure-controlled scanning calorimetry (PCSC) and Monte Carlo simulation to determine the methane inversion curve. They concluded that to figure out the complex behavior of the Joule-Thomson inversion curve with higher quality, a combination of experimental techniques and molecular simulations should be used.

Maghari and his colleagues [29] calculated the Joule-Thomson inversion curve using SAFT-CP equation of state for sixteen pure fluids, twelve of them were non-polar and four of them were polar fluids. They concluded that the SAFT-CP equation could predict the experimental data for non-polar fluids. In the case of polar fluids, low temperature branch predictions were satisfactory.

Haghighi and Bozorgnehr [30] used five recent equation of state to predict the Joule-Thomson inversion curve of some fluids (Argon, carbon dioxide, methane, ethane and butane). All of the five EOS were van der Walls type and they were: Wang-Gmehling (WG) EOS, modified Peng-Robinson by Twu-Coon-Cunnigham (PR-TCC) EOS, Riazi-Mansoori (RM) EOS, Geana EOS and modified Peng-Robinson-Stryjek-Vera proposed by Samir I. Abu- Eishah (PRSV2) EOS. They compared these EOS outcomes with experimental data and stated that the results were similar and most of EOS were more or less could predict low temperatures branch with the exception of RM equation. On the other hand, for higher temperatures they mostly failed. Haghighi and Bozorgmehr also determined these equations' maximum inversion pressure and temperature for every component used in their work.

Vrabec et al. [31] determined the Joule-Thomson inversion data of methane, ethane, nitrogen, carbon dioxide and their mixture with using molecular simulation and modeling. They compared these data with DDMIX, SUPERTRAPP, BACKONE and

GERG-2004 equations that were defined as the most advanced equation of state for computing inversion conditions. In addition to that the results of pure substances were compared to REFPROP data as a reference. They concluded their study with following results. Molecular modeling and simulation have similar result as BACKONE, which is an equation of state based on molecular simulation. SUPERTRAPP and DDMIX are not very reliable. They also stated that molecular simulation and modeling is the method of choice to predict Joule-Thomson inversion curve for mixture because no such complicated equation of state are available.

Abbas et al. [32] tested the reliability of the Joule-Thomson (JT) coefficient of the carbon dioxide, argon and some binary systems (carbon dioxide-argon and methane-ethane) using the group contributing equation of state VTPR. Besides, they calculated inversion condition of some compounds, their binary and ternary systems with this equation. They compared results of VTPR equation with available experimental data, corrected experimental data (REFPROP) and molecular simulation results of Vrabec et al. They found that attained results for JT coefficient and JT inversion curves were in resemblance with experimental findings.

Figueroa-Gerstenmaier et al. [33] identified molecular simulation methodology based on the NPH MC (Monte Carlo algorithm for fixed number of particles, specified pressure and enthalpy) to determine Joule-Thomson coefficient, Joule-Thomson inversion curve and isoenthalps for ethane-based refrigerants (R125, R134a and R152a) in wide range of thermodynamic conditions. Figueroa-Gerstenmaier et al. compared their simulation results with results obtained from the REFPROP software package and obtained good agreement. They also suggested that more precise quantum and statistical mechanical calculation of refrigerant would enhance the reliability of molecular simulation calculation of isoenthalps, Joule-Thomson coefficients and Joule-Thomson inversion data.

Nichita and Leibovici [34] calculated the Joule-Thomson inversion curve for two phase mixtures. The inversion curve for a mixture obtained by these authors using cubic equation of state (Soave-Redlich-Kwong and Peng-Robinson EOS). The Joule-Thomson inversion curve in the two-phase region is not a continuation of its single phase branch. There is a discontinuity at the phase envelope.

The latest study about prediction of Joule-Thomson inversion curve belong to Patankar and Atrey [35]. They calculated Joule-Thomson inversion curve for mixture of

nitrogen-methane and nitrogen-methane-carbon dioxide using Peng-Robinson, Redlich-Kwong and Soave-Redlich-Kwong equations of state and compared these results with Vrabec et al.'s molecular modeling and simulation results. The calculations were performed assuming single-phase conditions. Patankar and Atrey also constructed inversion curves of pure hydrogen and neon with trying different acentric factor values and stated that inversion condition calculated for pure fluids could be improved by choosing a proper value of acentric factor.

In Doğan's [36] study, Joule-Thomson inversion curve were computed using two, two-parameter equation of states written in reduced forms (van der Walls and Redlich-Kwong) and a reduced form z-factor correlation (Dranchuk-Abou Kassem). The results were compared against the experimental data published in the literature to figure out the effectiveness of the two parameter equations in prediction of Joule-Thomson inversion curve

Dilsiz [37] examined the derivative behavior of z-factor correlations by using thermophysical properties (residual enthalpy and entropy). She used Dranchuk-Abou Kassem and Hall-Yarborough correlations to calculate the thermophysical properties with different mixing rules. Moreover, she investigated effect of the mixing rules on the prediction of residual properties.

Since the inversion data are limited in the literature (especially for the upper section of the curve), several correlations, EOS based prediction methods, and molecular simulation techniques are used to compute inversion conditions of various gases. With the exception of some molecular simulation applications, none of these methods is able to predict inversion conditions accurately because the methods used in predictions are not suitable for high reduced temperature and pressure conditions.

3. MOTIVATION AND PURPOSE OF STUDY

Proper knowledge of the Joule-Thomson effect is necessary for many petroleum and natural gas engineering applications. However, direct measurement of inversion conditions requires precisely controlled experimental conditions. As a result of experienced difficulties in the experimental setups, the inversion data are limited in literature. In lack of adequate experimental data, some prediction methods are used to compute the inversion characteristics of different fluids. However, none of these methods is able to predict the inversion conditions accurately.

The main purpose of this study is to examine the applicability of three two-parameter (T_r and P_r) corresponding state type z-factor correlations (Dranchuk-Abou Kassem, Dranchuk-Purvis-Robinson, and Hall-Yarborough) in prediction of Joule-Thomson inversion curve. Adjustable parameters of these correlations should be optimized to improve the accuracy of the inversion curve computations. In accordance with this purpose, the details of the methodology used for improving predictions will be given in following chapter of this thesis.

In parameter estimation chapter, the parameters of the Dranchuk-Abou Kassem and Hall-Yarborough correlations are optimized by keeping the functional forms using all available experimental data and reference data including methane-ethane binaries (up to 10 per cent ethane) together to predict inversion conditions adequately. The optimization data mainly consist of reference data since experimental data is very limited especially in the high temperature branch of the inversion curve.

The experimental data are taken from Perry's chemical engineering handbook [38] which are concentrate on the lower inversion zone and Bessieres et al.'s study [28] which are concentrate on maximum pressure region, the reference data are taken from REFPROP reference program. All these data set are given in Appendix B. Moreover, the Matlab codes used in this study are given in Appendix A.

4. MODELING OF JOULE-THOMSON EFFECT

Temperature change of a gas upon volumetric change is modelled with Joule-Thomson coefficient. In this section, Joule-Thomson experiment, mathematical formulation of the Joule-Thomson coefficient, and Joule-Thomson inversion curve are explained.

4.1 Joule-Thomson effect

Joule-Thomson effect is a thermodynamic phenomenon that takes place when a fluid passes through a restriction. This throttling process usually accompanied with a change in temperature under isenthalpic conditions.

Joule-Thomson effect was discovered in an experiment conducted by James Joule and William Thomson in 1852 [39]. In the experiment, they supplied gas at steady rate (constant rate) through a tube that are separated into two parts with a porous plug and, the whole system is isolated from the surroundings to prevent heat exchange. The apparatus of Joule-Thomson experiment is shown in the Figure 1.1. Pistons are moved in the same direction to create pressure differences between separated parts. The pressure at the upstream side of the restriction is kept higher than the downstream part to ensure controlled expansion inside the porous plug.

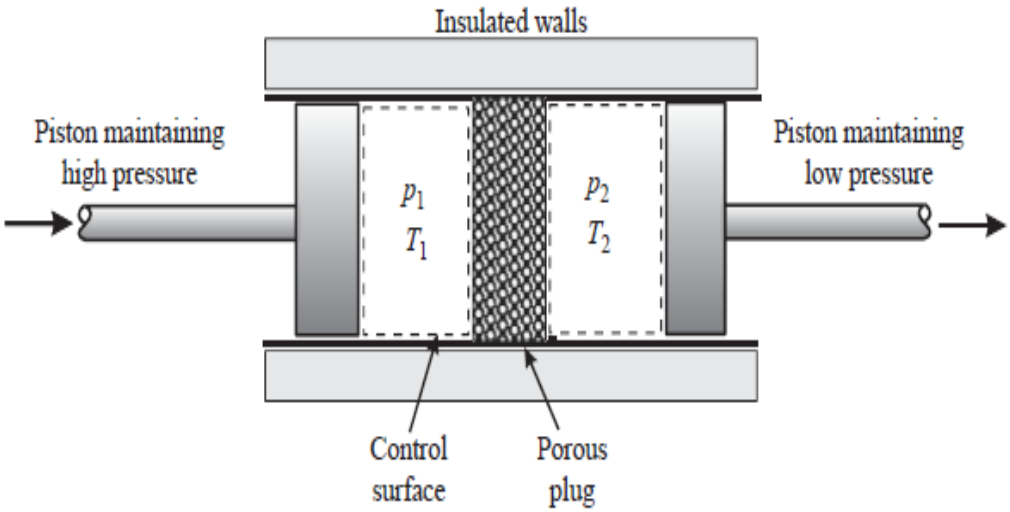

Figure 4.1: Joule-Thomson experiment apparatus.[40]

During the experiment, the gas occupies a volume V_1 at pressure P_1 and temperature T_1 before the expansion and a volume V_2 at pressure P_2 and temperature T_2 after the expansion.

The total work done by system can be defined as the summation of work done by the pistons.

$$w = -\int_{V_1}^{0} P_1 dV - \int_{0}^{V_2} P_2 dV = P_1V_1 - P_2V_2 \tag{4.1}$$

From the first law of thermodynamics, change in internal energy is equal to work done by system since there is no heat exchange between the apparatus and the surroundings:

$$\Delta U = U_2 - U_1 = w \tag{4.2}$$

$$U_2 - U_1 = P_1V_1 - P_2V_2 \tag{4.3}$$

$$U_1 + P_1V_1 = U_2 + P_2V_2 \tag{4.4}$$

By definition of enthalpy (H= U+PV), Equation 4.4 can be written as $H_1 = H_2$ and this equation shows that enthalpy of the system is unchanged. Therefore, this procedure is an isenthalpic expansion and the experiment measures the change in temperature of gas with the change in pressure at constant enthalpy. On a temperature-pressure graph, the Joule-Thomson process can be sketched as an isenthalpic curve (Figure 4.2). The line ABC shows the effect of decreasing the exit pressure on the exit temperature. The point B is known as the inversion pressure.

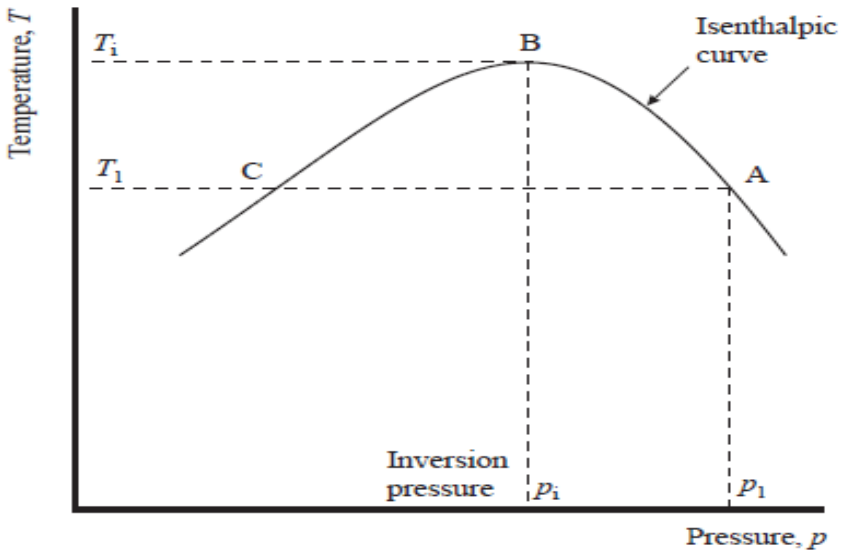

Figure 4.2: Isenthalpic curve for flow through a porous plug.[40]

According to Figure 4.2, direction of temperature change depends on the initial condition of pressure and temperature. Another words, temperature change could be in decreasing or increasing direction. This signed change of temperature during throttling process is modelled using the Joule-Thomson coefficient. Joule-Thomson coefficient represent the slope of the constant enthalpy line at P-T plane:

$$\mu_{JT} = \left(\frac{\partial T}{\partial P}\right)_H \tag{4.5}$$

The enthalpy constraint on the partial derivative may be converted to the measurable coordinates using the chain rule:

$$\left(\frac{\partial H}{\partial T}\right)_P \left(\frac{\partial T}{\partial P}\right)_H \left(\frac{\partial P}{\partial H}\right)_T = -1 \tag{4.6}$$

$$\left(\frac{\partial T}{\partial P}\right)_H = -\left(\frac{\partial H}{\partial P}\right)_T \left(\frac{\partial T}{\partial H}\right)_P \tag{4.7}$$

$$\mu_{JT} = \left(\frac{\partial T}{\partial P}\right)_H = \frac{\left(\frac{\partial H}{\partial P}\right)_T}{\left(\frac{\partial H}{\partial T}\right)_P} \tag{4.8}$$

By knowing that

$$dH = TdS + VdP \tag{4.9}$$

The pressure derivative of enthalpy may be written as

$$\left(\frac{\partial H}{\partial P}\right)_T = T\left(\frac{\partial S}{\partial P}\right)_T + V \tag{4.10}$$

The partial derivative of entropy can be replaced by its equivalent using the Maxwell equations.

$$\left(\frac{\partial S}{\partial P}\right)_T = -\left(\frac{\partial V}{\partial T}\right)_P \tag{4.11}$$

Then the pressure derivative of enthalpy becomes

$$\left(\frac{\partial H}{\partial P}\right)_T = -T\left(\frac{\partial V}{\partial T}\right)_P + V \tag{4.12}$$

On the other hand, temperature derivative of enthalpy has a special name of constant pressure heat capacity

$$C_P = \left(\frac{\partial H}{\partial T}\right)_P \tag{4.13}$$

The final expression for Joule-Thomson coefficient may be written as

$$\mu_{JT} = \frac{1}{C_P}\left[T\left(\frac{\partial V}{\partial T}\right)_P - V\right] \tag{4.14}$$

4.2 Joule-Thomson Inversion Curve

If Joule-Thomson experiment is repeated for different set of inlet pressure and temperatures and results of experiment are plotted at P-T plane as a constant enthalpy lines, the inversion points of these lines will construct the Joule-Thomson inversion curve. Intersection of the ordinate and inversion curve is called maximum inversion temperature as shown in Figure 4.3.

Inside the inversion curve where the Joule-Thomson coefficient is positive ($\mu_{JT} > 0$), the gas temperature decreases as a result of expansion (equivalently temperature increases as a result of compression). Outside the inversion curve where the coefficient is negative ($\mu_{JT} < 0$), expansion process increases the gas temperature (equvalently temperature decreases with decreasing volume).

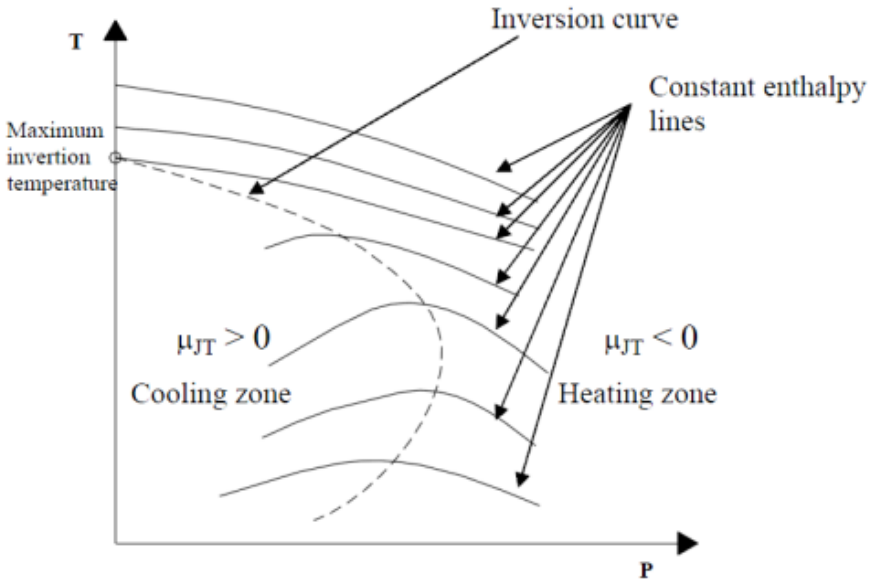

Figure 4.3: Joule-Thomson inversion curve and constant enthalpy lines.[41]

If the Joule-Thomson coefficient is identically zero, no temperature change will be observed as result of the volume change. Projection of P-T pairs at which the Joule-Thomson coefficient becomes identically zero creates an envelop on the P-T plane. This envelop is known as the Joule-Thomson inversion curve. The inversion curve seperates the P-T plane into two regions where the temperature changes have opposite effects.

5. CORRESPONDING STATE PRINCIPLE AND PREDICTION OF JOULE-THOMSON INVERSION CURVE

The details of method used for predicting the Joule-Thomson inversion curve using two parameters corresponding state z-factor correlations will be given in this section. Additionally, REFPROP reference software used to produce inversion curve data is introduced.

5.1 Corresponding State Principle

Corresponding state principle was developed by J. D. van der Walls for the first time. van der Walls showed that all pure substances' pressure, volume and temperature properties can be explained with two parameters equation of states in theoretically. For different substances, quantitative pressure-volume relations are not similar at constant temperature. However, according to corresponding state principle, when the reduced pressure and volume are taken as reference parameters for pressure, volume and temperature relationship of single component gases, two different substances which have similar structures show resembling properties. Corresponding state principle can be expressed in following equation generally.

$$f\left(\frac{P}{P_c},\frac{V}{V_c},\frac{T}{T_c}\right) = f\left(P_r,V_r,T_r\right) \cong 0 \tag{5.1}$$

where

P: System pressure

P_r: Reduced pressure

P_c: Critical pressure

T: System temperature

T_r: Reduced temperature

T_c: Critical temperature

V: System volume

V_r: Reduced volume

V_c: Critical volume

5.1.1 Reduced parameters

For single component gases, critical point is the end point of vapour pressure curve. The pressure and temperature are called as critical temperature and critical pressure at this point. The gases having same reduced values show similar physical behaviour. This is the basic rule of the corresponding states principle. The basic parameters of corresponding state principle are reduced pressure and reduced temperature. The expression of reduced parameters is given below:

$$T_r = T / T_c \tag{5.2}$$

$$P_r = P / P_c \tag{5.3}$$

Where system properties (Temperature and Pressure) and critical properties should be expressed in the same unit.

5.2 Two Parameter Corresponding State z-Factor Correlations

The basis for the numerical hydrocarbon gas z-factor correlations is the graphical correction published by Standing and Katz in 1942 [39]. Among the many numerical z-factor correlations, Hall-Yarborough, Dranchuk-Purvis-Robinson, and Dranchuk-Abou Kassem equations are chosen for this study. According to Kareem et al [40], these three correlations, described in the following subsections, are extensively used in the petroleum industry for their accuracies and low maximum errors.

5.2.1 Hall-Yarborough correlation

In 1973, Hall and Yarborough [41] presented an equation of state that precisely represents Standing and Katz chart. This equation of state based on Staring-Carnahan equation of state, and equation parameters were obtained to match the Standing and Katz chart data. Hall-Yarborough equation is given in the following form;

$$z = \left[\frac{0.06125 P_{pr} t}{Y} \right] \exp[-1.2(1-t)^2] \tag{5.4}$$

In Equation 5.4, t represents the inverse of reduced temperature value

$$t = \frac{T_{pc}}{T} \tag{5.5}$$

where T_{pc} represent pseudo-reduced temperature and Y represents reduced density that can be obtained from as the solution of the following equation.

$$\begin{aligned} F(Y) = &-0.06125 P_{pr} t \exp(-1.2(1-t)^2) + \frac{Y + Y^2 + Y^3 - Y^4}{(1-Y)^3} - \\ &(14.76t - 9.76t^2 + 4.58t^3)Y^2 + (90.7t - 242.2t^2 + 42.4t^3)Y^{(2.18+2.82t)} = 0 \end{aligned} \tag{5.6}$$

where P_{pr} is pseudo-reduced temperature.

The derivative of Equation 5.6 with respect to reduced density (Y) is given in following equation.

$$\begin{aligned} \frac{\partial f(Y)}{\partial Y} = &\frac{1 + 4Y + 4Y^2 - 4Y^3 + Y^4}{(1-Y)^4} - \left(29.52t - 19.52t^2 + 9.16^3\right)Y \\ &+ (2.18 + 2.82t)(90.7t - 242.2t^2 + 42.2t^3)Y^{(1.18+2.82t)} \end{aligned} \tag{5.7}$$

This non-linear equation could be solved with Newton-Raphson iterative method and the value of reduced density can be found. According to Tarek [45], this method is recommended for application if the pseudo-reduced temperature is higher than one.

5.2.2 Dranchuk-Purvis-Robinson method

Dranchuk, Purvis and Robinson [46] published a correlation based on the Benedict-Webb-Rubin equation of state. Developed correlation has eight parameters and these parameters were obtained using Standing and Katz chart using non-linear regression analysis. The equation has following form:

$$\begin{aligned} z = 1 &+ \left[A_1 + \frac{A_2}{T_{pr}} + \frac{A_3}{T_{pr}^3}\right]\rho_r + \left[A_4 + \frac{A_5}{T_{pr}}\right]\rho_r^2 + \left[\frac{A_5 A_6}{T_{pr}}\right]\rho_r^5 \\ &+ \left[\frac{A_7}{T_{pr}^3}\rho_r^2\left(1 + A_8\rho_r^2\right)\exp(-A_8\rho_r^2)\right] \end{aligned} \tag{5.8}$$

where ρ_r is reduced gas density and given by Equation 5.9.

$$\rho_r = \frac{0.27 P_{pr}}{z T_{pr}} \tag{5.9}$$

Parameters which are used in the Equation 5.8 are given in Table 5.1.

Table 5.1: Parameters of Dranchuck-Purvis-Robinson Method

Coefficient	Coefficient Values
A_1	0.31506237
A_2	-1.0467099
A_3	-0.57832729
A_4	0.53530771
A_5	-0.61232032
A_6	-0.10488813
A_7	0.68157001
A_8	0.68446549

Dranchuk-Purvis-Robinson method is operative within the following ranges;

$0.2 \leq P_{pr} \leq 30$

$1.05 \leq T_{pr} \leq 3.0$

Dranchuk-Purvis-Robinson equation is a precursor of Dranchuk-Abou Kassem equation.

5.2.3 Dranchuk-Abou Kassem correlation

Dranchuk and Abou Kassem correlation [47] is one of the two parameters corresponding state correlations. Dranchuk and Abou Kassem correlation has 11 parameters to simulate Standing and Katz chart. In this equation, z-factor may be written in terms of reduced parameters as follows:

$$z = \left[A_1 + \frac{A_2}{T_{pr}} + \frac{A_3}{T_{pr}^3} + \frac{A_4}{T_{pr}^4} + \frac{A_5}{T_{pr}^5} \right] \rho_r + \left[A_6 + \frac{A_7}{T_{pr}} + \frac{A_8}{T_{pr}^2} \right] \rho_r^2 - A_9 \left[\frac{A_7}{T_{pr}} + \frac{A_8}{T_{pr}^2} \right] + A_{10} \left(1 + A_{11} \rho_r^2 \right) \frac{\rho_r^2}{T_{pr}^3} \exp(-A_{11} \rho_r^2) + 1 \tag{5.10}$$

where ρ_r is reduced gas density defined in Equation 5.9.

Equation 5.10 includes the z value at the both side of equation, therefore; it must be solved iteratively. The constant coefficients in Equation 5.10 are obtained with nonlinear regression analysis and calculated with matching 1500 data point from

Standing and Katz chart. According to Tarek [45], Dranchuk-Abou Kassem equation can be employed in the range of $1.0 < T_{pr} < 3.0$ for reduced temperature and $0.2 \leq P_{pr} \leq 30.0$ for reduced pressure and gives results with 0.585 percentage error. Parameters which are used in the Equation 5.10 are given in Table 5.2.

Table 5.2: Parameters of Dranchuck-Abou Kassem Correlation

Coefficient	Coefficient Values
A_1	0.3265
A_2	-1.0700
A_3	-0.5339
A_4	0.01569
A_5	-0.05165
A_6	0.5475
A_7	-0.7361
A_8	0.1844
A_9	0.1056
A_{10}	0.6134
A_{11}	0.7210

5.3 REFPROP Reference Program

REFPROP reference program developed by the National Institute of Standards and Technology (NIST) and, this program provides thermodynamic and transport properties of fluids and fluid mixture.

REFPROP [48] data is calculated by the most precise pure fluid and mixture models currently applicable. Equation of state explicit in Helmholtz energy, the modified Benedict-Webb-Rubin equation of state and extended corresponding states (ECS) model are implemented by REFPROP for the thermodynamic properties of pure fluids. Mixture computation uses a model that employs mixing rule to the Helmholtz energy of the mixture components; it uses a separation function to account for the separation from ideal mixing.

REFPROP contains GERG-2008 and AGA-8 which are standards employed in the natural gas industry. GERG-2008 [46] is the equation of state for the thermodynamic properties of natural gases, this equation based on 21 natural gas component some of them are methane, nitrogen, carbon dioxide. The normal range of validity of GERG-2008 includes temperatures from (90 to 450) K and pressure up to 35 MPa where the most certain experimental data of the caloric and thermal features are represented to

within their accuracy. The extended range reaches from 60 to 700 K for temperature and up to 70 MPa for pressure. GERG-2008 will be adopted as an ISO Standard (ISO 20765-2/3) for natural gases.

5.4 Prediction of Inversion Curve

Measurement of Joule-Thomson inversion curve requires precisely controlled experimental conditions. As a result of experienced difficulties in experimental setups, the inversion data is limited in literature. In lack of sufficient experimental data some correlations, equation state based prediction methods and molecular simulation techniques are all used to compute inversion characteristic for different gases.

In the present study for predicting inversion characteristic, three of two parameters corresponding state type z-factor correlations are used. These are Dranchuk-Abou Kassem (DAK) correlation, Hall-Yarborough (HY) correlation and Dranchuk-Purvis-Robinson (DPR) correlation.

As mentioned before, Joule-Thomson inversion curve creates an envelope on the P-T plane that separates the regions at which the gases are either cooling or heating. On the inversion curve, the Joule-Thomson coefficient is identically zero.

In the previous chapter, the Joule-Thomson coefficient was written in terms of the constant pressure heat capacity, pressure, molar volume and temperature. In Equation 4.14, partial derivative of volume with respect to temperature can be rearranged using real gas equation on one mole basis:

$$PV = zRT \tag{5.11}$$

$$\left(\frac{\partial V}{\partial T}\right)_P = \frac{\partial}{\partial T}\left(\frac{zRT}{P}\right)_P = \frac{R}{P}\frac{\partial}{\partial T}\left(zT\right) \tag{5.12}$$

$$\left(\frac{\partial V}{\partial T}\right)_P = \frac{R}{P}\left[T\left(\frac{\partial z}{\partial T}\right)_P + z\right] \tag{5.13}$$

If this expression is inserted into the Joule-Thomson coefficient equation, the following will be obtained.

$$\mu_{JT} = \frac{1}{C_P}\left[\frac{RT^2}{P}\left(\frac{\partial z}{\partial T}\right)_P + \frac{zRT}{P} - V\right] \tag{5.14}$$

Equation 5.14 can be simplified as follows:

$$\mu_{JT} = \frac{RT^2}{PC_P}\left(\frac{\partial z}{\partial T}\right)_P \tag{5.15}$$

In the right-hand side of Equation 5.15, R, T, P, and Cp are all positive and the sign of the Joule-Thomson coefficient is controlled by the partial derivative of the z-factor. Equation 5.15 may be written in terms of reduced parameters if the following conversions are made:

$$T = T_{pr}T_{pc} \tag{5.16}$$

$$P = P_{pr}P_{pc} \tag{5.17}$$

$$dT = T_{pc}dT_{pr} + T_{pr}dT_{pc} \tag{5.18}$$

$$dP = P_{pc}dP_{pr} + P_{pr}dP_{pc} \tag{5.19}$$

Since dT_{pc} and dP_{pc} terms are identically equal to zero, Equation 5.15 is expressed in reduced parameters as follow:

$$\mu_{JT} = \frac{RT_{pr}{}^2T_{pc}}{P_{pr}P_{pc}C_P}\left(\frac{\partial z}{\partial T_{pr}}\right)_{P_{pr}} \tag{5.20}$$

Since at the Joule-Thomson inversion point, μ_{JT} becomes zero, Equation 5.20 is reduced to the following simpler form:

$$\left(\frac{\partial z}{\partial T_{pr}}\right)_{P_{pr}} = 0 \tag{5.21}$$

At this point inversion curve may be computed in terms of reduced properties. The two-parameters corresponding states z-factor correlations based on the Standing-Katz chart. Our primary concern in this study is to compare temperature derivative properties of Dranchuk-Abou Kassem and Hall Yarborough correlations. Dranchuk-Purvis-Robinson correlation is also used since this correlation is a precursor of the Dranchuk-Abou Kassem equation.

To compute the inversion curve the following steps are taken:

As the first step, all three equations are coded as functions of reduced properties. Since all three equations have z-factor at both sides of the correlation equations, Newton-Raphson algorithm is used to solve the non-linear equations. The code is also modified to run with Matlab's *fzero* function to check correctness of our code. The *fzero* [50] function uses a combination of bisection, secant and inverse quadratic interpolation methods.

As the second step, the derivatives are evaluated numerically by using central differences method with a step size of 0.0001. Analytical derivatives of the equations were also taken and compared to validate the results. There is no significant changes in the results when the numerical derivatives are used.

Finally, as the third step, Equation 5.21 is solved by using Matlab's *fzero* function T_{pr} starting from 1.01 to 5.0 with 0.1 increments. This type of calculation is very similar to the phase envelope calculations in vapor-liquid equilibria. Since reduced pressure can take two values for a given reduced temperature value, the iteration variable has to be taken as the reduced pressure. The currently computed reduced pressure value is taken as the initial guess for the next iteration step.

Initially, methane data is used to compare the results. The experimental data were taken from Perry's Chemical Engineering handbook [38] and Bessieres et al.'s [28] study. Since most of the data available is concentrated on the low temperature range of the curve, REFPROP reference program is also employed.

REFPROP reference program can compute the thermodynamic properties as a function of pressure and temperature. If pure component data is required, those thermodynamic properties may be retrieved in terms of reduced properties. The reference program has no options to compute the inversion points. To overcome this problem, the Joule-Thomson coefficient is computed as a function of reduced pressure while reduced temperature is held constant. Then, the turnover point is refined in a much narrower temperature range. The point at which μ_{JT} changes the sign is the inversion point.

Figure 5.1 shows calculated inversion data from Dranchuk-Abou Kassem correlation for methane, experimental data and inversion data from REFPROP reference program. Cross plot of predicted versus reference values of inversion pressure is given in Figure 5.2.

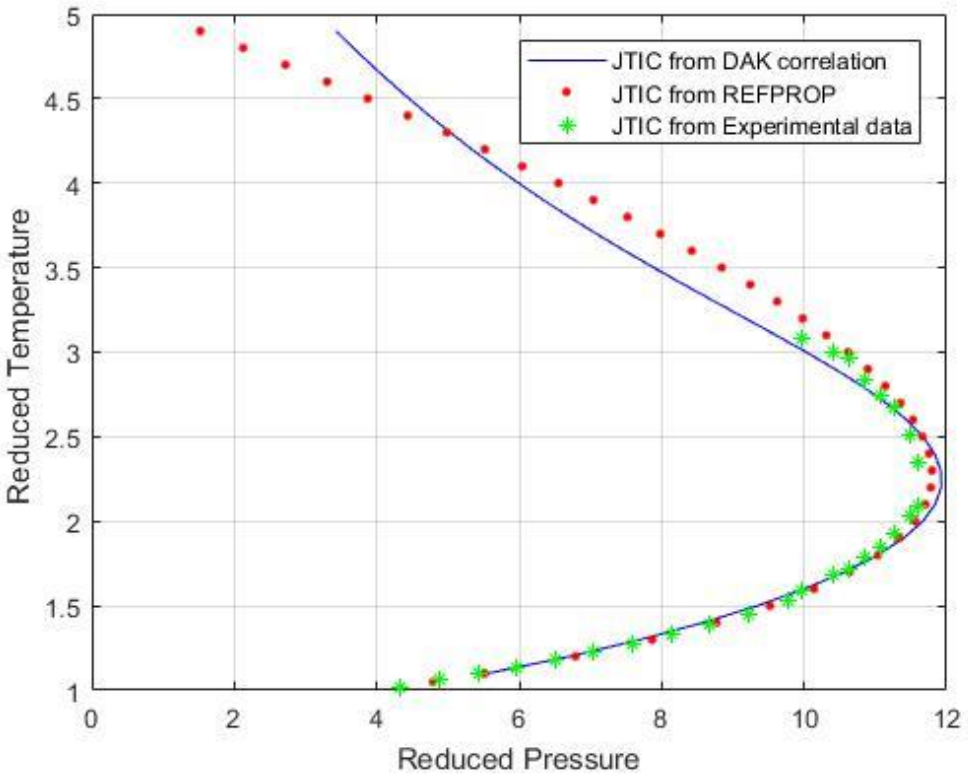

Figure 5.1: Inversion curve from DAK correlation calculated with original coefficients.

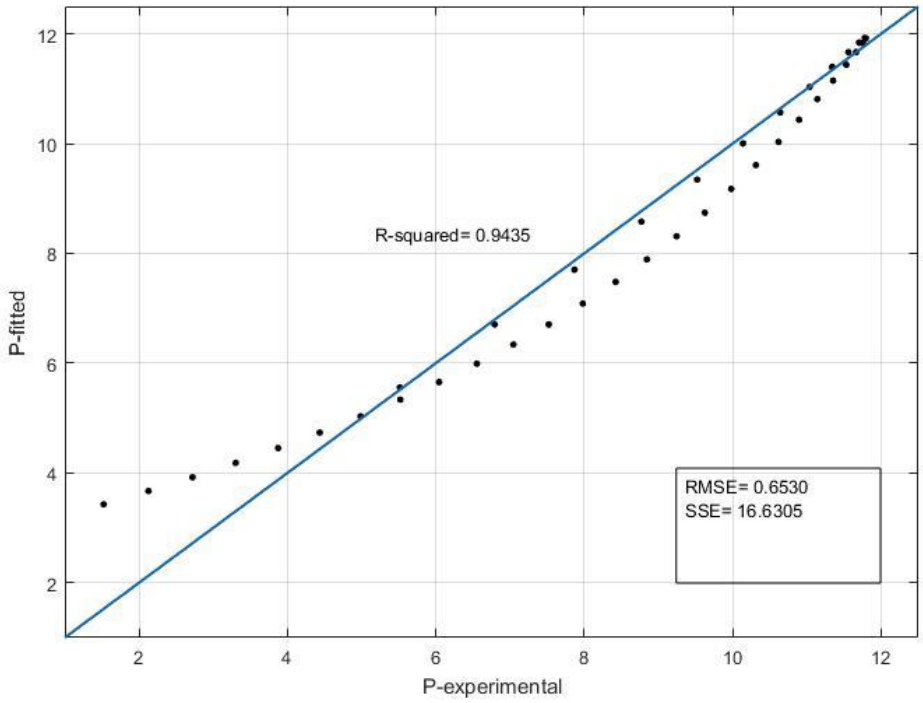

Figure 5.2: Cross plot of predicted by DAK vs. reference values of inversion pressure.

Figure 5.1 shows that the experimental and the REFPROP data are in close agreement at the low temperature branch of the inversion curve. DAK correlation slightly underestimates the experimental data. Incompatibility increases at the maximum pressure region and above 2.5 value of reduced temperature, resemblance completely disappears. The functional form of the correlation is not capable of following the experimental data. It should be noted that upper temperature limit for the correlation is 3.0.

Figure 5.3 shows that Hall-Yarborough correlation represent an acceptable agreement at the lower branch of the inversion curve but underestimates the middle and upper branch up to T_{pr} value of 4. Functional form of the correlation is in closer agreement with the experimental data compared to the DAK correlation. Figure 5.4 shows the comparison of the inversion pressures that are measured by Hall-Yarborough correlation and reference inversion pressure.

Finally Figure 5.5 shows the predictions of DPR correlation. Since the correlation is simpler form of the DAK correlation similar conclusions are valid. The difference between the DPR correlation predictions and the reference data is larger. Figure 5.6 shows the comparison of the inversion pressures that are measured by DPR correlation and reference inversion pressure.

Figure 5.7 reveals that none of the correlations used in this study can predict entire curve. DAK and DPR correlations can predict the lower branch of the inversion curve in close agreement while HY correlation has a more robust shape but fail to predict the curve in the maximum pressure and temperature regions.

As a final conclusion of this chapter, Dranchuk-Abou Kassem and Hall-Yarborough correlation coefficients should be optimized to improve the inversion curve predictions without changing the original form of the correlations.

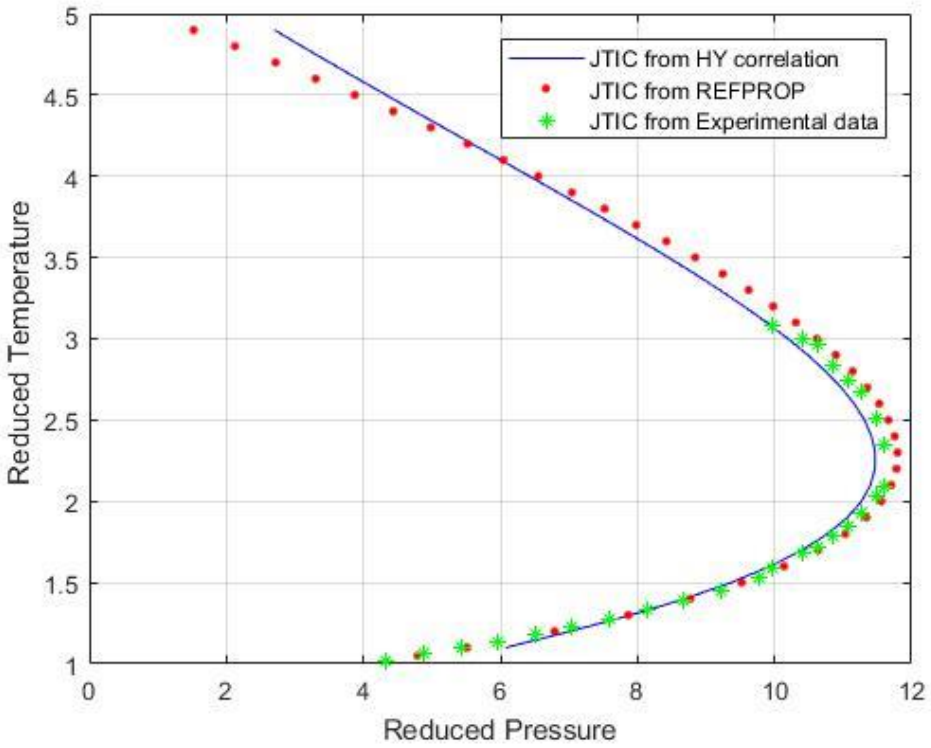

Figure 5.3: Inversion curve from HY correlation calculated with original coefficients.

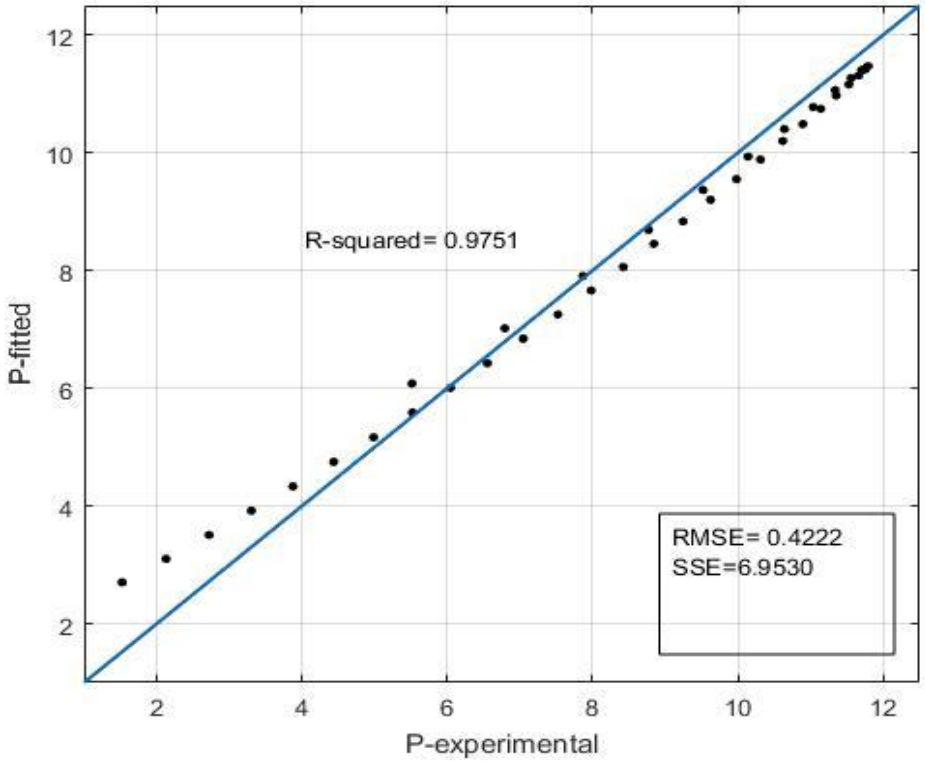

Figure 5.4: Cross plot of predicted by HY vs. reference values of inversion pressure.

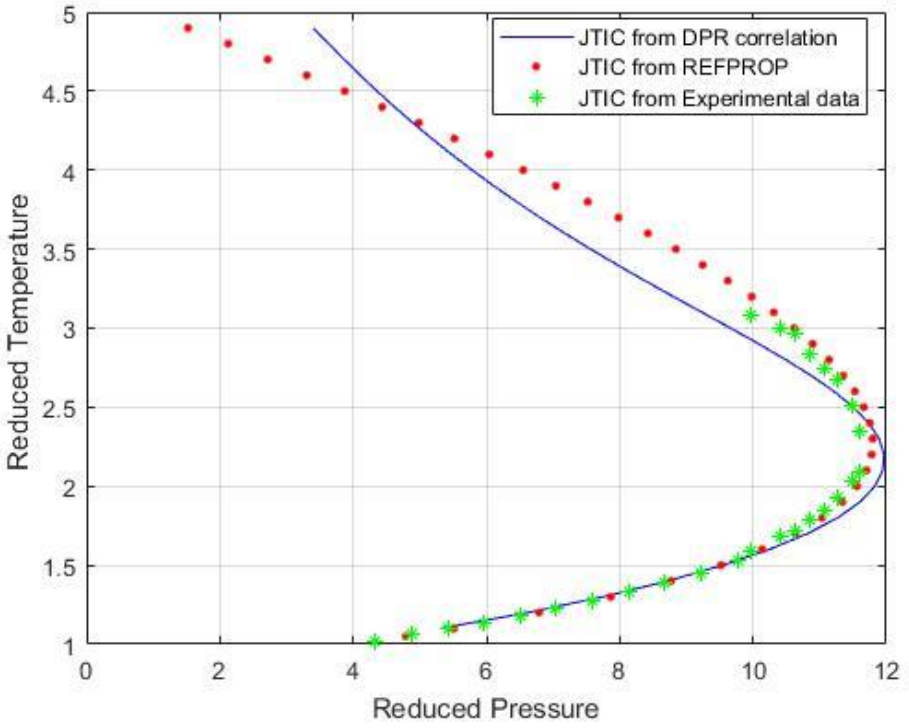

Figure 5.5: Inversion curve from DPR correlation calculated with the original coefficients.

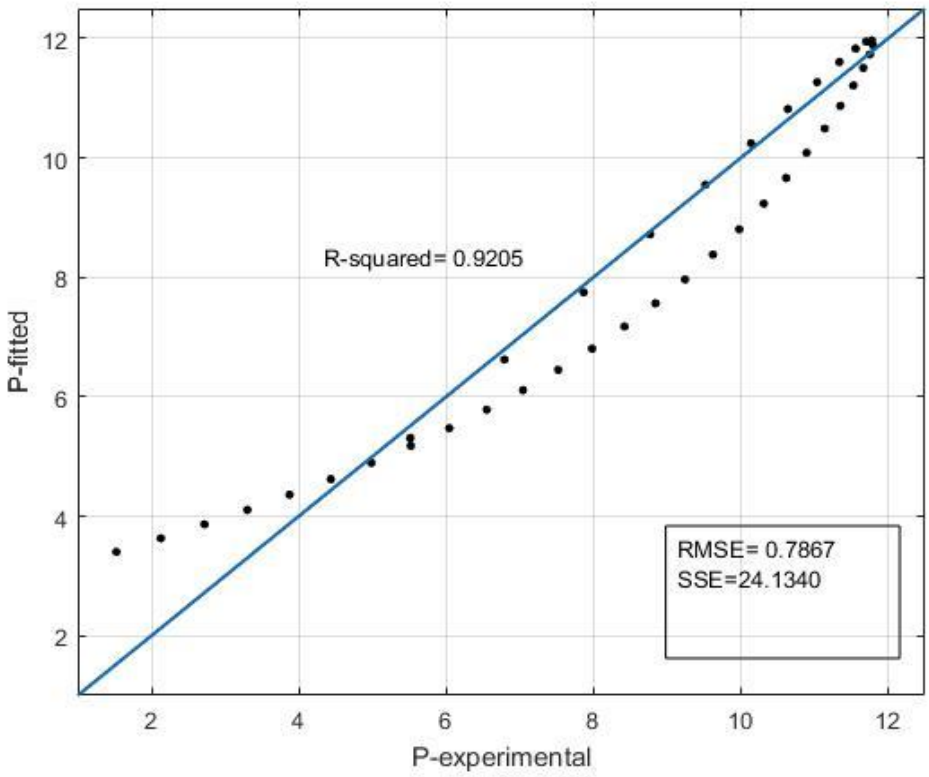

Figure 5.6: Cross plot of predicted by DPR vs. reference values of inversion pressure.

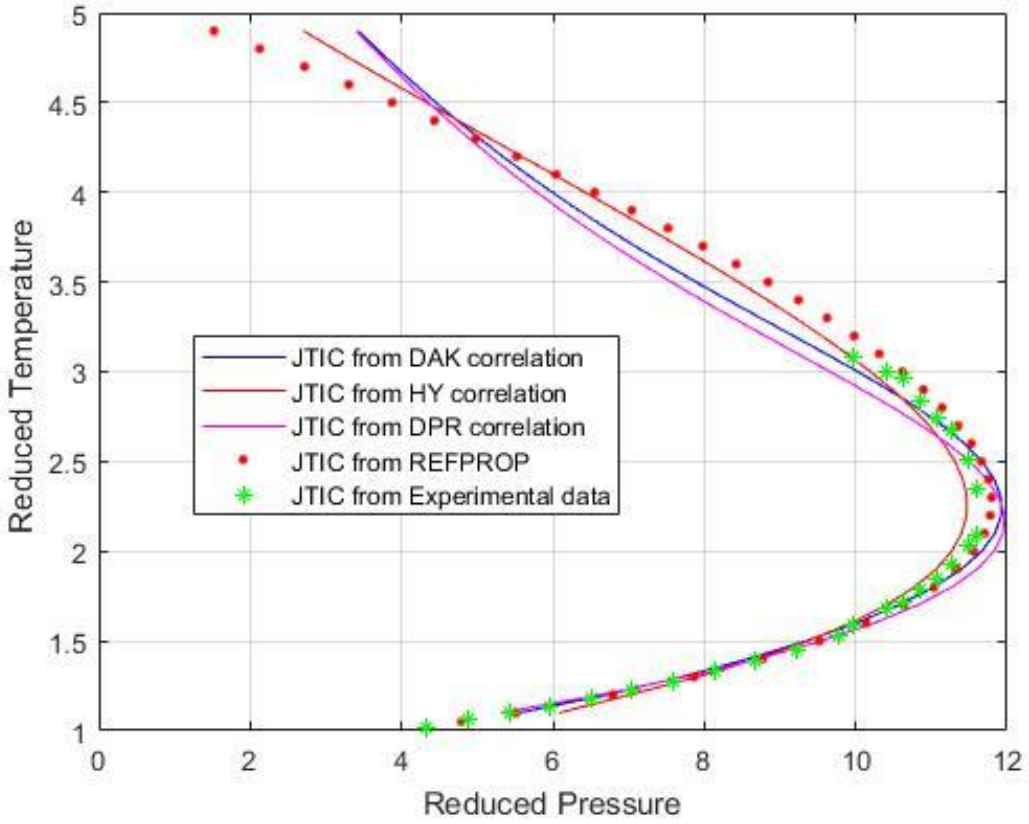

Figure 5.7: Comparison of the three correlations.

6. PARAMETER ESTIMATION

Prediction of the Joule-Thomson inversion curve by using the z-factor correlations based on the Katz's chart was found inadequate especially in the high temperature branch as proved in the previous chapter of this thesis.

In this chapter, the parameters of the DAK and HY equations are optimized by keeping the functional forms of the z-factor correlations using reference data including methane-ethane binaries (up to 10 per cent ethane) from REFPROP and experimental data from literature. This type of approach is especially preferable to make the previously developed codes usable and predict full range of inversion curve adequately. The optimization data comes mainly from REFPROP reference program, since data is very limited especially in the high temperature branch of the curve.

The differences between the reference and predicted data are calculated using sum of squares error (SSE). Sum of squares error of prediction, also known as the residual sum of squares, is the sum of squares of residuals. It is a measure of the inconsistency between the data and the assumed model. A small SSE shows a close fitting of the model to the data. SSE is used as an optimality criterion in parameter and model selection.

According to Drapper and Smith [51], In model with single descriptive variable, SSE is given by:

$$SSE = \sum_{i=1}^{n} \left(y_i - f(x_i) \right)^2 \tag{6.1}$$

Where y_i is the ith value of the variable to be estimated, x_i is the ith value of the descriptive variable, and $f(x_i)$ is the predicted value of y_i.

In this work, MATLAB's optimization routines are used for parameter optimization keeping the functional forms unchanged. MATLAB's ***fminsearch*** function uses Nelder and Mead (NM) (or simplex search algorithm) originally published in 1965 [52]. NM algorithm is designed for multidimensional unconstrained optimization

without using the derivatives. The method uses four different procedures to find the minimum: reflection, expansion, contraction, and shrink. The inner working of the algorithm is out of scope of this study and may be find somewhere else such as Nash J.C. [53].

6.1 Parameter Estimation for Dranchuk-Abou Kassem Correlation

All available experimental and reference data is used with equal weight to regress the DAK correlation. The regression results are given in Table 6.1. R-squared value for this optimization run is 0.9951. Cross plot of the data and predictions are given in Figure 6.1. The agreement between the values are acceptable in the low-temperature region of the curve. In the maximum inversion pressure region and high-temperature section of the curve, the agreement is still requires an improvement. The new coefficients over-estimates the data in the maximum pressure region while there are positive and negative deviations in the upper part of the curve. The functional form of the DAK correlation cannot predict the entire curve precisely with one set of coefficients.

Table 6.1: Parameters of DAK correlation estimated by using reference data.

Coefficient	Coefficient Values
A_1	0.372857
A_2	-0.963299
A_3	-0.797675
A_4	0.015154
A_5	-0.077576
A_6	0.230204
A_7	-0.150227
A_8	-0.040879
A_9	0.308500
A_{10}	0.776886
A_{11}	0.800990

To increase the precision of the predictions, inversion curve data is divided into two parts and new parameters for each part are re-optimized. In order to do keep continuity, common data points for both data sets are used.

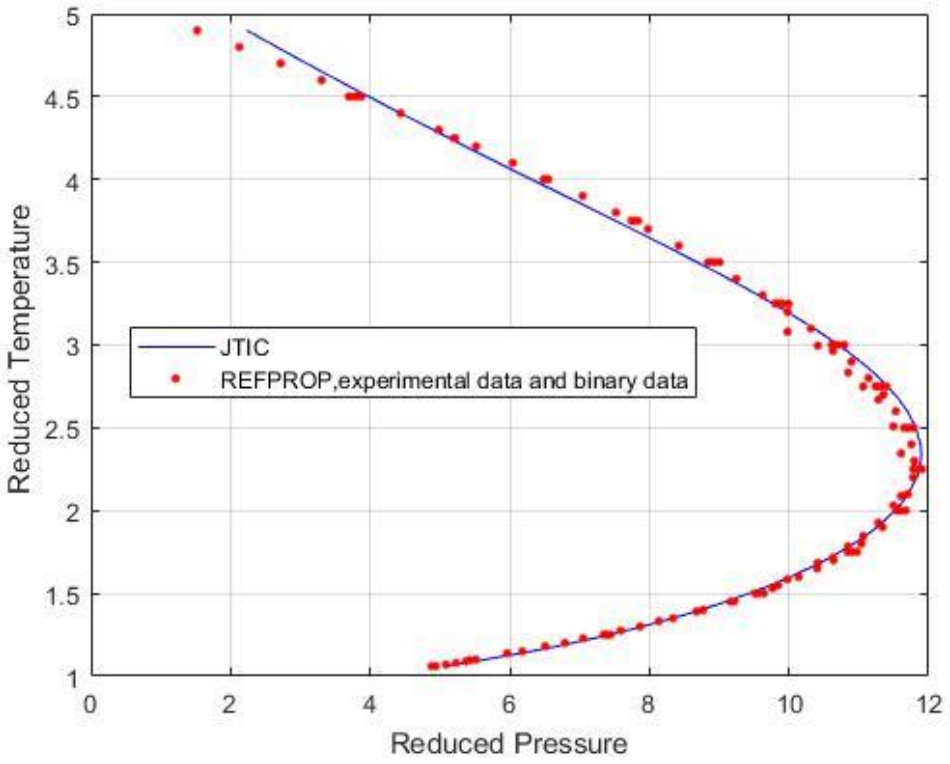

Figure 6.1: Inversion curve from DAK correlation calculated with new optimized one-set coefficients.

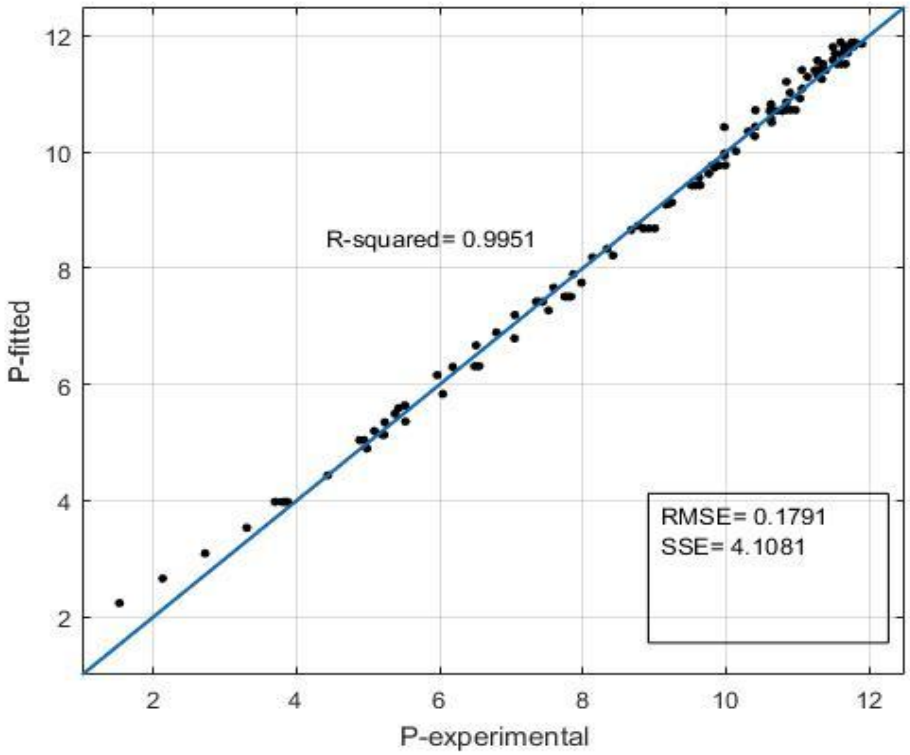

Figure 6.2: Cross plot of predicted vs. reference values of inversion pressure for DAK correlation (one parameter set).

The weighted SSE values are determined with following equation:

$$SSE = \sum_{i=1}^{n} \left(w_i (y_i - f(x_i)) \right)^2 \tag{6.2}$$

where, w_i are the weights of data points i.

In two sets of optimization for DAK correlation, the point with reduced temperature value 2.9 is used as a weighted point to keep continuity.

To determine parameters of DAK correlation for lower inversion curve, the data that are chosen in range of $1.05 < T_r \leq 2.9$ are used. The results are given in Table 6.2.

The same procedure is applied for upper inversion curve, with using reference data in range of $2.9 \leq T_r < 4.9$ and obtained new parameters are tabulated in Table 6.3.

Table 6.2: Parameters of DAK correlation for lower inversion curve.

Coefficient	Coefficient Values
A_1	0.216104
A_2	-1.192575
A_3	-0.579851
A_4	0.015341
A_5	-0.055257
A_6	0.604008
A_7	-0.679496
A_8	0.191558
A_9	0.093118
A_{10}	0.692834
A_{11}	0.732255

Table 6.3: Parameters of DAK correlation for upper inversion curve.

Coefficient	Coefficient Values
A_1	0.397296
A_2	-1.005186
A_3	-0.429393
A_4	0.015362
A_5	-0.052815
A_6	0.199828
A_7	-0.291067
A_8	0.243582
A_9	0.142355
A_{10}	1.045814
A_{11}	0.830423

Lower and upper inversion curves are computed separately with using parameters in Table 6.2 and Table 6.3 and the results are plotted in Figure 6.3 and Figure 6.4. The final plot including both curves are shown in Figure 6.5, the cross plot of the experimental, and predicted values are shown in Figure 6.6. In Figure 6.5, the continuous green line is the upper inversion curve and obtained with using parameters tabulated in Table 6.3. The continuous blue line represents the lower inversion curve and it is determined with using parameters in Table 6.2. As shown in the figure the inversion curve generated by two-segment correlation shows the excellent agreement with the data in all regions (R-squared value is 0.9990).

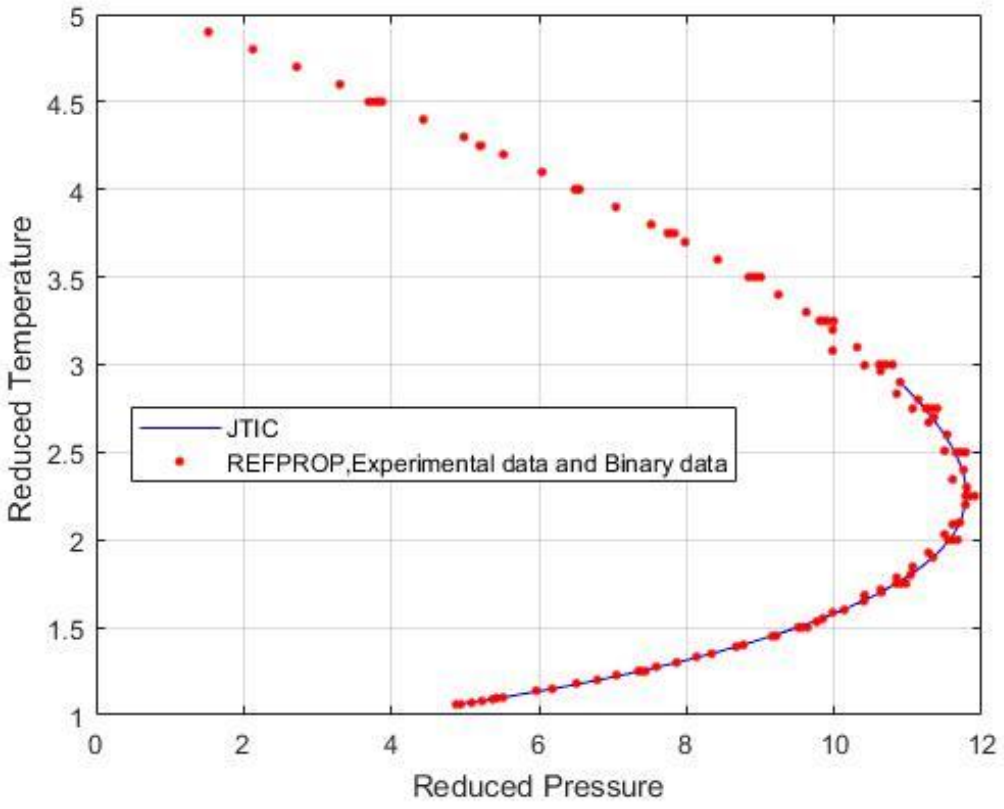

Figure 6.3: Lower inversion curve from DAK correlation calculated with optimized parameters.

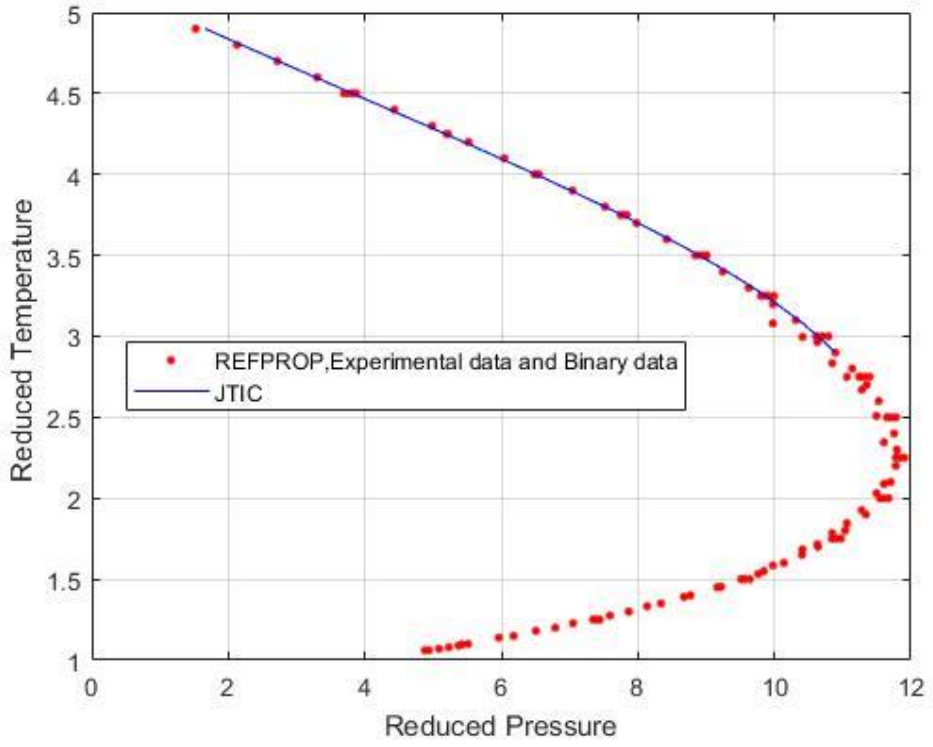

Figure 6.4: Upper inversion curve from DAK correlation calculated with optimized parameters.

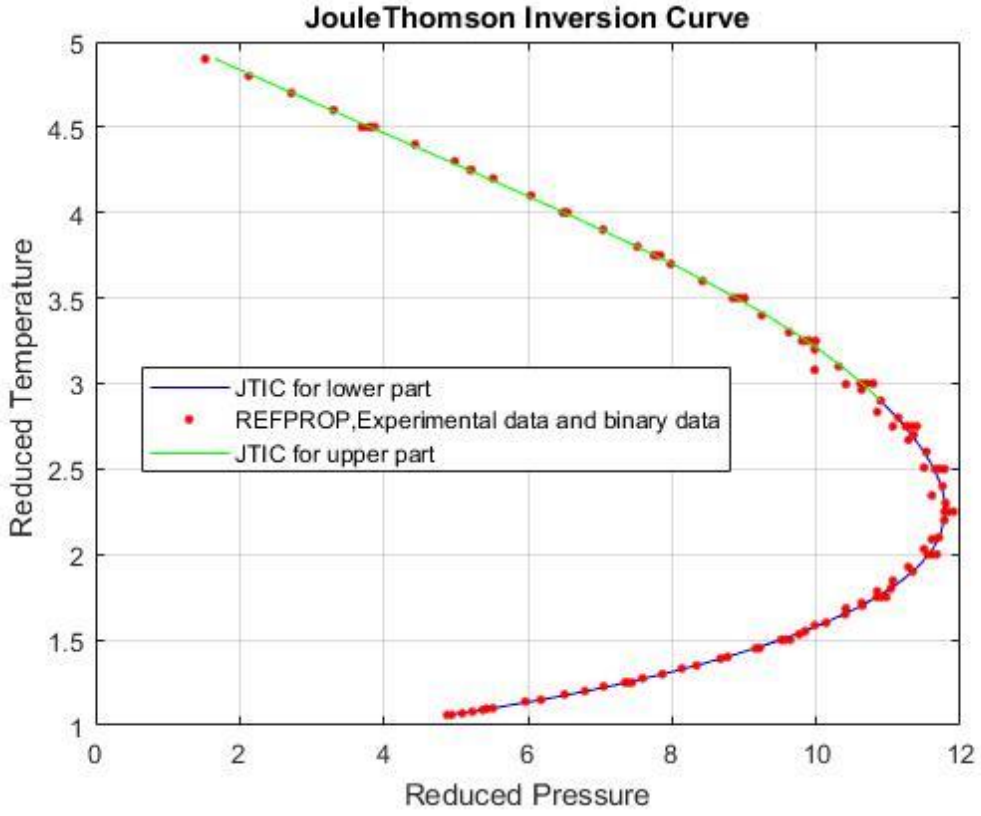

Figure 6.5: Lower and upper inversion curve from DAK correlation.

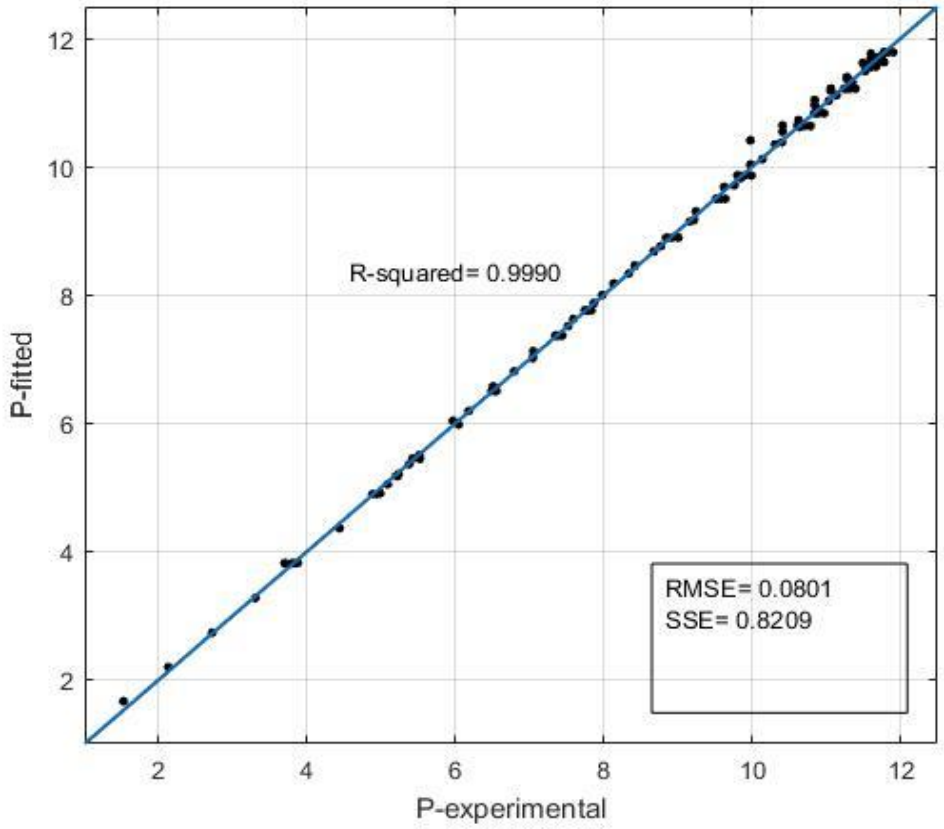

Figure 6.6: Cross plot of measured vs. reference and experimental data with two sets coefficients.

6.2 Parameter Estimation for Hall-Yarborough Correlation

In order to estimate new parameters without disturbing the structure of Hall-Yarborough correlation, HY correlation is written in the following form.

$$F(Y) = -0.06125 P_{pr} t \exp(-1.2(1-t)^2) + \frac{Y + Y^2 + Y^3 - Y^4}{(1-Y)^3} - (C_1 t - C_2 t^2 + C_3 t^3) Y^2 + (C_4 t - C_5 t^2 + C_6 t^3) Y^{(C_7 + C_8 t)} = 0 \quad (6.3)$$

Where, C1-C8 are parameters which should be estimated in the HY correlation.

As in the DAK correlation, these parameters are found because of the minimization of SSE values between the reference data and the predicted data.

Table 6.4 shows the estimated parameters of Hall-Yarborough correlation.

Table 6.4: Parameters of HY correlation estimated by using reference data.

Coefficient	Coefficient Values
C_1	13.037330
C_2	5.404216
C_3	5.158509
C_4	77.022020
C_5	282.777973
C_6	46.918170
C_7	2.543076
C_8	3.234061

Figure 6.7 shows the Joule-Thomson inversion curve from HY correlation calculated with above parameters. As it can be seen from the figure that HY correlation shows good prediction capabilities in all regions of the inversion curve with the new coefficients.

Figure 6.8 indicates, cross plot of measured inversion pressures versus reference inversion pressures.

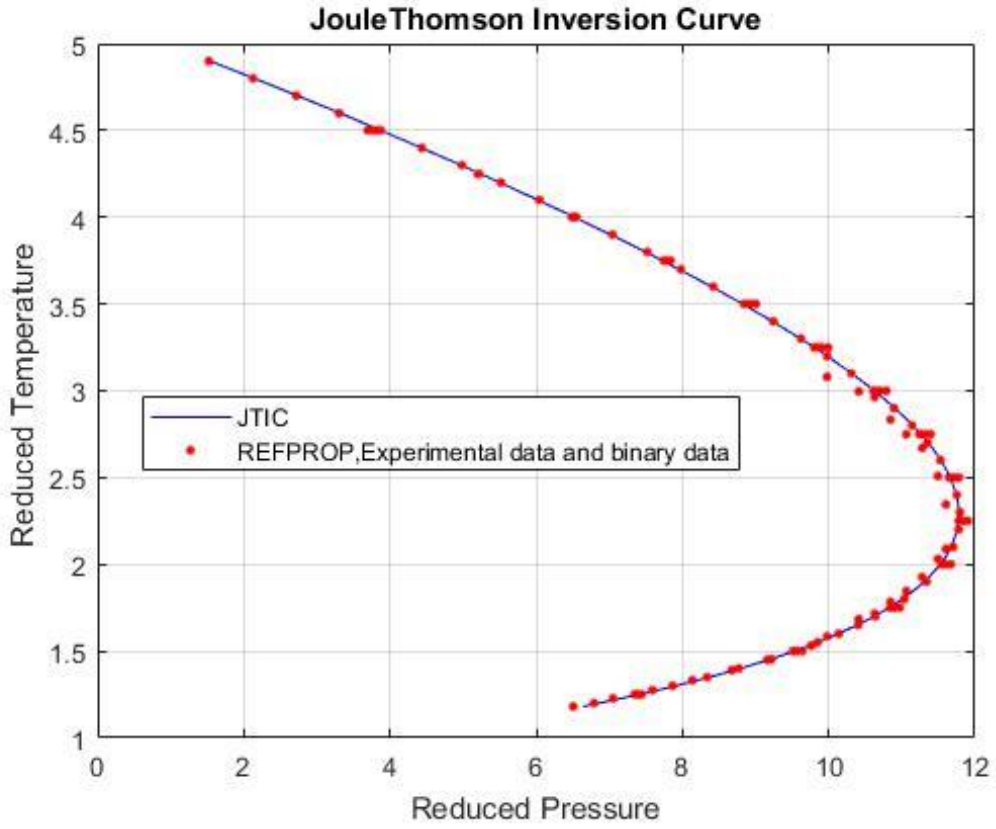

Figure 6.7: Inversion curve from HY correlation calculated with new optimized coefficients.

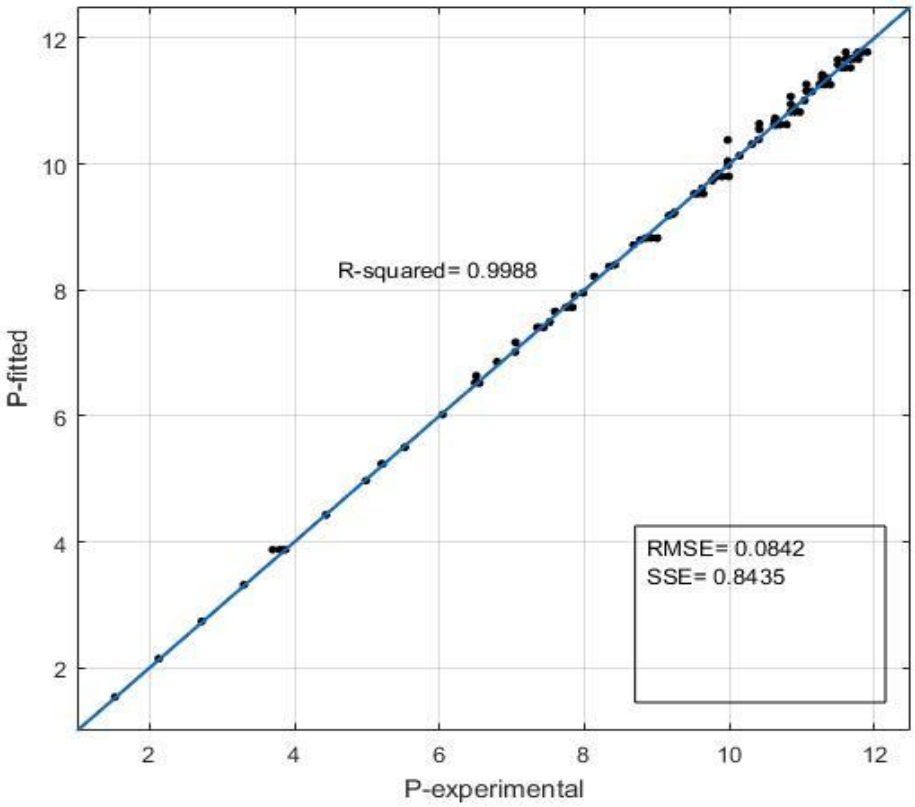

Figure 6.8: Cross plot of measured vs. reference and experimental data for HY correlation.

According to Figure 6.7 and Figure 6.8, Hall-Yarborough correlation can be reliably used to predict inversion curve of natural gases with high methane percentage. There is no need optimization for Hall-Yarborough correlation by separating two parts since this correlation gives results adequately.

7. CONCLUSIONS

The main purpose of this thesis is to test the capability of the z-factor correlations based on the Katz's z-factor data in predicting the Joule-Thomson inversion curve and then optimize the parameters to improve the predictions as necessary. The following conclusions are reached at the end of this study:

1. Joule-Thomson inversion curve is computed for Dranchuk-Abou Kassem, Dranchuk-Purvis-Robinson and Hall-Yarborough correlations. All three correlations give reasonable results in the lower inversion branch. On the other hand, these correlations were failed in upper inversion branch and at the peak point of inversion curve. Hall-Yarborough correlation shows better agreement at the high temperature region.

2. Parameters of Dranchuk-Abou Kassem correlation is optimized by using experimental and REFPROP reference data including methane-ethane binaries (up to 10 per cent ethane). New coefficients give more accurate results than non-optimized version of Dranchuk-Abou Kassem correlation. Yet more improvements are necessary at the maximum inversion pressure region and high temperature branch of the curve.

3. To improve the predictions from Dranchuk-Abou Kassem equation, inversion curve data is divided into two parts ($1.05 < Tr < 2.9$ & $2.9 \leq Tr < 4.9$) and new parameter sets are estimated. The resulting correlation with two sets of parameters has a R-squared value of 0.9990 which is an indication of close fit.

4. Hall-Yarborough correlation has a better functional conformance compare to Dranchuk-Abou Kassem equation. The reference and experimental data can be predicted with the Hall-Yarbrough with a single set of optimized parameters. The coefficients of reciprocal of the reduced temperature are chosen while keeping the original form of the equation.

5. We expect that the new optimized parameters will improve the enthalpy calculations using these two correlations. However, this conclusion is yet to be proved in another study.

REFERENCES

[1] **Jones, C.** (1988, January). The use of bottomhole temperature variations in production testings. In European Petroleum Conference. Society of Petroleum Engineers.

[2] **Baker, A. C., & Price, M**. (1990, January). Modelling the performance of high-pressure high-temperature wells. In European Petroleum Conference. Society of Petroleum Engineers.

[3] **B. Yadali Jamaloei, K. Asghari.** (2015). The Joule-Thomson Effect in Petroleum Fields: I.Well Testing, Multilateral/Slanted Wells, Hydrate Formation, and Drilling/Completion/Production Operations, Energy Sources, Part A: Recovery, Utilization, and Environmental Effect, 37:2

[4] **B. Yadali Jamaloei, K. Asghari.** (2015). The Joule-Thomson Effect in Petroleum Fieds: II. CO_2 Sequestration, Wellbore Temperature Profiles, and Thermal Stresses and Wellbore Stability, Energy Sources, Part A: Recovery, Utilization, and Environmental Effect, 37:3

[5] **Pakulski, M.** (2007). Accelerating effect of surfactants on gas hydrates formation. International Symposium on Oilfield Chemistry, Houston, TX, February 28-March 2.

[6] **Batesole, E.C., Wilkes, J.O.** (1988). Thermal effect in cyclic operation of storage reservoirs. SPE reservoir engineering, 3(04), 1-295

[7] **Oldenburg, C.M.** (2007). Joule-Thomson cooling due to CO2 injection into natural gas reservoirs. *Energy Conversion and Management*, *48*(6), 1808-1815.

[8] **Steffensen,R.J., Smith,R.C.** (1973). The importance of Joule-Thomson heatin(or cooling) in temperature log interpretation. In Fall Meeting of Society of Petroleum Engineers of AIME. Society of Petroleum Engineers.

[9] **App, J.F.** (2010). Nonisothermal and productivity behavior of high pressure reservoirs.*SPE J.* 15:50-63.

[10] **Roebuck, J.R. Osterberg, H.** (1933). The Joule Thomson effect in helium. Physical Review, 43(1), 60.

[11] **Roebuck, J.R. Osterberg, H.** (1934). The Joule Thomson effect in argon. Physical Review, 46(9), 785.

[12] **Roebuck, J.R. Osterberg, H.** (1935). The Joule Thomson effect in nitrogen. Physical Review, 48(5), 450.

[13] **Budenholzer, R.A. Sage, B.H. Lacey W.N.** (1939). Phase equilibria in Hydrocarbon Systems. Industrial & Engineering Chemistry, 31(3), 369-374

[14] **Gunn, R.D., Chueh, P.L., &Prausnitz, J.M.** (1966). Inversion temperatures and pressures for cryogenic gases and their mixtures. Cryogenics, 6(6), 324-329

[15] **Miller, D. G.** (1970). Joule Thomson inversion curve, corresponding state, and simpler equation of state. Industrial & Engineering Chemistry Fundamentals, 9(4), 585-589

[16] **Dilay, G. W., Heidemann, R.A.** (1986). Calculation of Joule-Thomson inversion curves from equation of state. Industrial & engineering chemistry fundamentals, 25(1), 152-158.

[17] **Colaza, A. V., Da Silva, F.A., Müller, E.A., Olivera-Fuentes, C.** (1962). Joule-Thomson Inversion Curves and Supercritical Cohesion Parameters of Cubic Equation of State. Lat. Am. Appl. Res, 22, 135.

[18] **Maghari, A., Matin, N. S.** (1997). Prediction of Joule Thomson inversion curves from van der Walls type equation of state. Journal of chemical engineering of Japan, 30(3), 520-525

[19] **Darwih, N. A., Al-Muhtaseb, S. A.** (1996). A comparison between four cubic equation of state in predicting the inversion curve and spinodal curve loci of methane. Thermochimica acta, 287(1), 43-52

[20] **Colina, C, M., Olivera-Fuentes, C.** (1998). Prediction of the Joule-Thomson inversion curve of air from cubic equation of state. Cryogenics, 38(7), 721-728.

[21] **Castillo, M.G., Colina, C.M., Dubuc, J. E., Olivera-Fuentes, C.G.** (1999). Three-Parameter Corresponding-States Correlations for Joule-Thomson Inversion Curves. International journal of thermophysics, 20(6), 1737-1751

[22] **Matin, N. S., Haghighi, B.** (2000). Calculation of the Joule-Thomson inversion curves from cubic equation of state. Fluid phase equilibria, 175(1-2), 273-284

[23] **Colina, C. M., Müller, E. A.** (1999). Molecular simulation of Joule-Thomson Inversion Curves. International journal of thermophysics, 20(1), 229-235.

[24] **Chacın, A., Vázquez, J. M., & Müller, E. A.** (1999). Molecular simulation of the Joule–Thomson inversion curve of carbon dioxide. Fluid Phase Equilibria, 165(2), 147-155.

[25] **Colina, C. M., Turrens, L. F., Gubbins, K. E., Olivera-Fuentes, C., & Vega, L. F.** (2002). Predictions of the Joule− Thomson Inversion Curve for the n-Alkane Series and Carbon Dioxide from the Soft-SAFT Equation of State. Industrial & engineering chemistry research, 41(5), 1069-1075.

[26] **Haghighi, B., Laee, M. R., & Matin, N. S.** (2003). A comparison among five equations of state in predicting the inversion curve of some fluids. Cryogenics, 43(7), 393-398.

[27] **Vrabec, J., Kedia, G. K., & Hasse, H.** (2005). Prediction of Joule–Thomson inversion curves for pure fluids and one mixture by molecular simulation. Cryogenics, 45(4), 253-258.

[28] **Bessières, D., Randzio, S. L., Pineiro, M. M., Lafitte, T., & Daridon, J. L.** (2006). A Combined Pressure-controlled Scanning Calorimetry and Monte Carlo Determination of the Joule− Thomson Inversion Curve. Application to Methane. The Journal of Physical Chemistry B, 110(11), 5659-5664.

[29] **Maghari, A., Safaei, Z., & Sarhangian, S.** (2008). Predictions of the Joule–Thomson inversion curves for polar and non-polar fluids from the SAFT-CP equation of state. Cryogenics, 48(1-2), 48-55.

[30] **Haghighi, B., & Bozorgmehr, M. R.** (2012). Joule-Thomson inversion curves calculation by using equation of state. Asian Journal of Chemistry, 24(2), 533.

[31] **Vrabec, J., Kumar, A., & Hasse, H.** (2007). Joule–Thomson inversion curves of mixtures by molecular simulation in comparison to advanced equations of state: Natural gas as an example. Fluid phase equilibria, 258(1), 34-40.

[32] **Abbas, R., Ihmels, C., Enders, S., & Gmehling, J.** (2011). Joule–Thomson coefficients and Joule–Thomson inversion curves for pure compounds and binary systems predicted with the group contribution equation of state VTPR. Fluid phase equilibria, 306(2), 181-189.

[33] **Figueroa-Gerstenmaier, S., Lísal, M., Nezbeda, I., Smith, W. R., & Trejos, V. M.** (2014). Prediction of isoenthalps, Joule–Thomson Coefficients and Joule–Thomson inversion curves of refrigerants by molecular simulation. Fluid Phase Equilibria, 375, 143-151.

[34] **Nichita, D. V., & Leibovici, C. F**. (2006). Calculation of Joule–Thomson inversion curves for two-phase mixtures. Fluid phase equilibria, 246(1-2), 167-176.

[35] **Patankar, A. S., & Atrey, M. D.** (2017, February). Construction of Joule Thomson inversion curves for mixtures using equation of state. In IOP Conference Series: Materials Science and Engineering (Vol. 171, No. 1, p. 012086). IOP Publishing.

[36] **Doğan, N. B.** (2004). Redlich-Kwong durum denklemleri kullanılarak Joule-Thomson tersinme eğrisinin bulunması. In Turkish (Undergraduate Desing Project, İstanbul Teknik Üniversitesi)

[37] **Dilsiz, E. A**. (2010). İki Farklı Z-faktörü Korelasyonu Türev Davranışlarının Artık Ve Termofiziksel Büyüklükler Kullanılarak İncelenmesi, In Turkish (Master Thesis, İTÜ Fen Bilimleri Enstitüsü).

[38] **Perry, R. H., Green, D. W., & Maloney, J. O.** (1997). Perry's chemical engineers' handbook.

[39] **Joule, J. P., & Thomson, W.** (1852). LXXVI. On the thermal effects experienced by air in rushing through small apertures. The London, Edinburgh, and Dublin Philosophical Magazine and Journal of Science, 4(28), 481-492.

[40] **Winterbone, Desmond E. Turan, Ali.** (2015). Advanced Thermodynamics for Engineers (2nd Edition). Elsevier.

[41] **Dalai, A.** (2012). Nitrogen and helium liquefer design and simulation using aspen plus. (Doctoral dissertation)

[42] **Standing, M. B., & Katz, D. L.** (1942). Density of natural gases. Transactions of the AIME, 146(01), 140-149.

[43] **Kareem, L. A., Iwalewa, T. M., & Al-Marhoun, M.** (2016). New explicit correlation for the compressibility factor of natural gas: linearized z-factor isotherms. Journal of Petroleum Exploration and Production Technology, 6(3), 481-492.

[44] **Hall, K. R., & Yarborough, L.** (1973). A new equation of state for Z-factor calculations. Oil Gas J, 71(25), 82.

[45] **Tarek, A.** (1993). Hydrocarbon Phase Behavior, Butterworth-Heinemann.

[46] **Dranchuk, P. M., Purvis, R. A., & Robinson, D. B.** (1973, January). Computer calculation of natural gas compressibility factors using the Standing and Katz correlation. In Annual Technical Meeting. Petroleum Society of Canada.

[47] **Dranchuk, P. M., & Abou-Kassem, H.** (1975). Calculation of Z factors for natural gases using equations of state. Journal of Canadian Petroleum Technology, 14(03).

[48] **Url-1.** <https://www.nist.gov/srd/refprop> date retrieved 09,.11.2018

[49] **Kunz, O., & Wagner, W.** (2012). The GERG-2008 wide-range equation of state for natural gases and other mixtures: an expansion of GERG-2004. Journal of chemical & engineering data, 57(11), 3032-3091.

[50] **Url-2.** <https://www.mathworks.com/help/matlab/ref/fzero.html> date retrieved 07,.11.2018

[51] **Drapper, N. R., & Smith, H.** (1998). Applied regression analysis. John Wiley & Sons.

[52] **Nelder, J. A., & Mead, R.** (1965). A simplex method for function minimization. The computer journal, 7(4), 308-313.

[53] **Nash, J. C.** (1990). Compact numerical methods for computers: linear algebra and function minimisation. CRC press.

APPENDICES

APPENDIX A: The Matlab code

APPENDIX B: The inversion data sets

APPENDIX A

```
clc;
clear all;
close all;

Tpr=1.1:0.1:4.9; %Tpr range

Ppri=4; %Initial Ppr values
for i=1:numel(Tpr)
P(i)=fzero(@num,Ppri,[],Tpr(i)); %DAK correlation

Phy(i)=fzero(@num2,Ppri,[],Tpr(i));%HY correlation

Pzp(i)=fzero(@num3,Ppri,[],Tpr(i));%DPR correlation
Ppri=P(i);
fprintf('%f\t%f\n',Tpr(i),P(i));
end

refprop=xlsread('JTIC.xlsx','methane','A2:B41');
expdata=xlsread('expJTIC.xlsx','Sheet1','R2:S28');



%JTIC from DAK,REFPROP and experimental data
figure
plot(P,Tpr,'b')
hold on
plot(refprop(:,2),refprop(:,1),'.r','MarkerSize',10)
hold on
plot(expdata(:,1),expdata(:,2),'*g')
grid on
xlabel('Reduced Pressure');
ylabel('Reduced Temperature ');
legend('JTIC from DAK correlation','JTIC from REFPROP','JTIC from Experimental
data');


%JTIC from HY,REFPROP and experimental data
figure
plot(Phy,Tpr,'b')
hold on
plot(refprop(:,2),refprop(:,1),'.r','MarkerSize',10)
hold on
plot(expdata(:,1),expdata(:,2),'*g')
grid on
xlabel('Reduced Pressure');
ylabel('Reduced Temperature ');
legend('JTIC from HY correlation','JTIC from REFPROP','JTIC from Experimental data');


%JTIC from DPR,REFPROP and experimental data
figure
```

```
plot(Pzp,Tpr,'b')
hold on
plot(refprop(:,2),refprop(:,1),'.r','MarkerSize',10)
hold on
plot(expdata(:,1),expdata(:,2),'*g')
grid on
xlabel('Reduced Pressure');
ylabel('Reduced Temperature ');
legend('JTIC from DPR correlation','JTIC from REFPROP','JTIC from Experimental
data');


%JTIC from DAK,HY,DPR,REFPROP and experimental data
figure
plot(P,Tpr,'b')
hold on
plot(Phy,Tpr,'r')
hold on
plot(Pzp,Tpr,'m')
hold on
plot(refprop(:,2),refprop(:,1),'.r','MarkerSize',10)
hold on
plot(expdata(:,1),expdata(:,2),'*g')
grid on
xlabel('Reduced Pressure');
ylabel('Reduced Temperature ');
legend('JTIC from DAK correlation','JTIC from HY correlation','JTIC from DPR
correlation','JTIC from REFPROP','JTIC from Experimental data');

% derivative term for DAK correlation
function [ f ] = num( Ppr,Tpr )
h=0.0001;
f=(zad(Tpr+h,Ppr)-zad(Tpr-h,Ppr))/(2*h);
end
function [ z ] = zad(Tpr,Ppr )
z=1;
 for i=1:100

A1=0.3265;  A2=-1.07;  A3=-0.5339;  A4=0.01569;
A5=-0.05165; A6=0.5475;  A7=-0.7361;  A8=0.1844;
A9=0.1056;  A10=0.6134;  A11=0.721;
Q=(0.27*Ppr)/Tpr;

D1=(A1+(A2/Tpr)+(A3/Tpr^3)+(A4/Tpr^4)+(A5/Tpr^5))*Q;
D2=(A6+(A7/Tpr)+(A8/Tpr^2))*Q^2;
D3=(A9*((A7/Tpr)+(A8/Tpr^2)))*Q^5;
D4=(A10/Tpr^3)*Q^2;
D5=(A10*A11/Tpr^3)*Q^4;
D6=-A11*Q^2;
D7=exp(D6*z^-2);
F=z-((D1*z^-1)+(D2*z^-2)-(D3*z^-5)+((D4*z^-2+D5*z^-4)*D7)+1);
Ft1=-D1*z^-2;
Ft2=-2*D2*z^-3;
Ft3=-5*D3*z^-6;
Ft4=(-2*D4*z^-3*D7)+(D4*z^-2*D7*-2*D6*z^-3);
Ft5=(-4*D5*z^-5*D7)+(D5*z^-4*D7*-2*D6*z^-3);
Ft=1-(Ft1+Ft2-Ft3+Ft4+Ft5);
```

```
correction=F/Ft;
if (abs(correction)<1.e-6);
    break;
end
z=z-correction;
 end
end

% derivative term for HY correlation

function [ f ] = num2( Ppr,Tpr )
h=0.01;
f=(hy(Tpr+h,Ppr)-hy(Tpr-h,Ppr))/(2*h);


end

function [ z] = hy( Tpr,Ppr )
y=0.00001;
t= 1/Tpr;

a=0.06125*t*exp(-1.2*(1-t)^2);

for i=1:100

  A1=(y+y^2+y^3-y^4)/(1-y)^3;
  A2= - (14.76*t-9.76*t^2+4.58*t^3);
  A3= (90.7*t - 242.2*t^2+42.4*t^3);
  A4= (2.18+2.82*t);

  B1= (1+4*y+4*y^2-4*y^3+y^4)/(1-y)^4;
  B2=29.52*t-19.52*t^2 +9.16 *t^3;
  B3= 2.18+2.82*t;
  B4= 90.7*t-242.2*t^2+42.4*t^3;
  B5= 1.18+ 2.82*t;


  f= -a*Ppr + A1 + A2*y^2 + A3*y^A4;
  fp= B1-B2*y+B3*B4*y^B5;

  corr=f/fp;

  if (abs(corr)<1.e-6);
      break
  end
  y=y-corr;
  z=a*Ppr*(1/y);
end


end
% derivative term for DPR correlation

function [ f ] = num3( Ppr,Tpr )
h=0.01;
f=(zdp2(Tpr+h,Ppr)-zdp2(Tpr-h,Ppr))/(2*h);
```

```
end

function [ z] = zdp2( Tpr,Ppr )
z=fzero(@zdp,1,[],Tpr,Ppr);
end
function [ f ] = zdp(z,Tpr,Ppr )


A1=0.31506237;  A2=-1.0467099;  A3=-0.57832720;  A4=0.53530771;
A5=-0.61232032; A6=-0.10488813;  A7=0.68157001;  A8=0.68446549;



T1=(A1+(A2/Tpr)+(A3/Tpr^3));
T2=(A4+(A5/Tpr));
T3=(A5*A6/Tpr);
T4=(A7/Tpr^3);
T5=(0.27*Ppr/Tpr);

Q=((0.27*Ppr)/(z*Tpr));
f=1+T1*Q+T2*Q^2+T3*Q^5+(T4*Q^2*(1+A8*Q^2)*exp(-A8*Q^2))-(T5/Q);
end
```

Parameter optimization code for DAK

```
clc;
clear all;
format short;
global model_Pr;


filename = 'wholebinary1.xlsx';
sheet = 1;
xlRange = 'A8:A135';
Trdata = xlsread(filename,sheet,xlRange);

sheet = 1;
xlRange = 'B8:B135';
Prdata = xlsread(filename,sheet,xlRange);

plot(Prdata,Trdata,'.r');
hold on;



fun = @(x) sse(x,Prdata,Trdata);
x0 = [0.3265;-1.07;-0.5339;0.01569;-0.05165;0.5475;-
0.7361;0.1844;0.1056;0.6134;0.7210];
fitcoef = fminsearch(fun,x0);

for i=1:11
    fprintf('A%d=\t%f;\n',i,fitcoef(i));
end

function [ f ] = num( Pr,Tr,coef )
```

```
h=0.0001;

f=(zad(Tr+h,Pr,coef) - zad(Tr-h,Pr,coef))/(2.0*h);


end

function [retval]= sse(coef,Prdata,Trdata)

for i= 1:numel(Trdata)
    Pr_ini= Prdata(i);
    Pr_inversion(i)= fzero(@num,Pr_ini,[],Trdata(i),coef);
end

sum= 0;
for i= 1:numel(Trdata)
    sum= sum + ((Prdata(i) - Pr_inversion(i)))^2;
end

retval= sum;
end

function [ z ]= zad( Tr,Pr,coef )
A1= coef(1);
A2= coef(2);
A3= coef(3);
A4= coef(4);

A5= coef(5);
A6= coef(6);
A7= coef(7);
A8= coef(8);

A9 = coef(9);
A10= coef(10);
A11= coef(11);

if (Pr < 1.E-20)
       z= 1.0;
       return;
end

z= 1.0;
z= zbeggs(Tr,Pr);
if(z < 0.)
    z= 0.2;
end


for i = 1:50

       Rhor= 0.27*Pr/(z*Tr);
       R2= Rhor*Rhor;

       c1= A1 + A2/Tr + A3/Tr^3. + A4/Tr^4. + A5/Tr^5.;
       c2= A6 + A7/Tr + A8/Tr^2.;
       c3= A9*(A7/Tr + A8/Tr^2.);
       c4= A10*(1.+A11*R2)*(R2/Tr^3.) * exp(-A11*R2);
```

```
        F = z - (1. + c1*Rhor + c2*R2 - c3*Rhor^5. + c4);

        dF= 1.+ c1*Rhor/z + 2.*c2*R2/z - 5.*c3*Rhor^5./z;
        dF= dF+2.*A10*R2*(1.+A11*R2-(A11*R2)^2.) * exp(-A11*R2)/(z*Tr^3.);

        correction = F / dF;

        if (abs(correction) <= 0.000001)
                return;
        end

    z = z - correction;

end

        z= 0.0;

end


function [z]= zbeggs(Tr,Pr)

E= 9.*(Tr-1.);

F= 0.3106 -0.49*Tr + 0.1824*Tr*Tr;

A= 1.39*(Tr-0.92)^0.5-0.36*Tr-0.1;

B= (0.62-0.23*Tr)*Pr + (0.066/(Tr-0.86)-0.037)*Pr*Pr + 0.32*Pr^6./(10.^E);

C= 0.132 - 0.32*log10(Tr);

D= 10.^F;

z= A + (1.-A)/exp(B) + C * Pr^D;

end
```

Parameter optimization code for HY

```
clc;
clear all;
format short;
global model_Pr;


filename = 'wholebinary1.xlsx';
sheet = 1;
xlRange = 'A17:A135';
Trdata = xlsread(filename,sheet,xlRange);

sheet = 1;
xlRange = 'B17:B135';
Prdata = xlsread(filename,sheet,xlRange);
```

```
plot(Prdata,Trdata,'.r');
hold on;


fun = @(x) sse(x,Prdata,Trdata);
x0 = [14.76,9.79,4.58,90.7,242.2,42.4,2.18,2.82];
fitcoef = fminsearch(fun,x0);

for i=1:8
    fprintf('C%d=\t%f;\n',i,fitcoef(i));
end


function [retval]= sse(coef,Prdata,Trdata)

for i= 1:numel(Trdata)
    Pr_ini= Prdata(i);
    Pr_inversion(i)= fzero(@num,Pr_ini,[],Trdata(i),coef);
end

sum= 0;
for i= 1:numel(Trdata)
    sum= sum + ((Prdata(i) - Pr_inversion(i)))^2;
end

retval= sum;
end

function [ f ] = num( Pr,Tr,coef )

h=0.0001;

f=(hy(Tr+h,Pr,coef) - hy(Tr-h,Pr,coef))/(2.0*h);

end

function [ z ] = hy( Tr,Pr,coef )
C1= coef(1);
C2= coef(2);
C3= coef(3);
C4= coef(4);

C5= coef(5);
C6= coef(6);
C7= coef(7);
C8= coef(8);

y=0.00001;
t= 1/Tr;
a=0.06125*t*exp(-1.2*(1-t)^2);

for i=1:1000

  A1=(y+y^2+y^3-y^4)/(1-y)^3;
  A2= -(C1*t-C2*t^2+C3*t^3);
  A3= (C4*t - C5*t^2+C6*t^3);
  A4= (C7+C8*t);
```

```
  B1= (1+4*y+4*y^2-4*y^3+y^4)/(1-y)^4;
  B2=(C1*t-C2*t^2 +C3*t^3)*2;
  B3= (C7+C8*t);
  B4= C4*t-C5*t^2+C6*t^3;
  B5= ((C7-1)+C8*t);


  f= -a*Pr + A1 + A2*y^2 + A3*y^A4;
  fp= B1-B2*y+B3*B4*y^B5;

  corr=f/fp;
  %disp(corr)
  if (abs(corr)<1.e-6);
      break
  end
  y=y-corr;
  z=a*Pr*(1/y);
end

end
```

APPENDIX B

Table B.1: Inversion data from REFPROP.

T_{pr}	P_{pr}	T_{pr}	P_{pr}
1.05	4.789789	2.75	11.39464
1.10	5.514308	2.80	11.14038
1.20	6.791620	2.90	10.89422
1.25	7.352904	3.00	10.61721
1.25	7.348367	3.00	10.61469
1.25	7.358536	3.00	10.63759
1.25	7.389108	3.00	10.70109
1.25	7.440140	3.00	10.7899
1.30	7.867568	3.10	10.31179
1.40	8.769778	3.20	9.980001
1.50	9.520768	3.25	9.805372
1.50	9.514813	3.25	9.830081
1.50	9.529152	3.25	9.898145
1.50	9.571409	3.25	9.992076
1.50	9.639614	3.30	9.623628
1.60	10.13903	3.40	9.244207
1.70	10.63993	3.50	8.84309
1.75	10.84201	3.50	8.843068
1.75	10.85733	3.50	8.865239
1.75	10.90236	3.50	8.925988
1.75	10.97304	3.50	9.006788
1.80	11.03641	3.60	8.421487
1.90	11.33952	3.70	7.98051
2.00	11.55885	3.75	7.746342
2.00	11.54777	3.75	7.76005
2.00	11.56288	3.75	7.79537
2.00	11.60618	3.75	7.834652
2.00	11.67254	3.80	7.521204
2.10	11.70280	3.90	7.044573
2.20	11.77887	4.00	6.551599
2.25	11.78145	4.00	6.532173
2.25	11.79648	4.00	6.531063
2.25	11.83912	4.00	6.522059
2.25	11.90247	4.00	6.488513
2.30	11.79375	4.10	6.043248
2.40	11.75348	4.20	5.52047
2.50	11.66345	4.30	4.984187
2.50	11.65266	4.40	4.435271
2.50	11.66916	4.50	3.874514
2.50	11.71545	4.50	3.828774
2.50	11.78225	4.50	3.796451
2.60	11.52850	4.50	3.697615
2.70	11.35289	4.60	3.302579
2.75	11.24386	4.70	2.719953
2.75	11.26341	4.80	2.126882
2.75	11.31772	4.90	1.523298

Table B.2: Inversion data from Bessieres et al.'s study.

T_{pr}	P_{pr}	T_{pr}	P_{pr}
1.584470	9.978308	2.345226	11.60521
1.684155	10.41215	2.507870	11.49675
1.715635	10.62907	2.670514	11.27983
1.783841	10.84599	2.749213	11.06291
1.846800	11.06291	2.833158	10.84599
1.925498	11.27983	2.964323	10.62907
2.030430	11.49675	2.995803	10.41215
2.088143	11.60521	3.079748	9.978308

Table B.3: Inversion data from Perry's Chemical Engineers' Handbook.

T_{pr}	P_{pr}	T_{pr}	P_{pr}
1.059811	4.880694	1.453305	9.219089
1.096537	5.422993	1.532004	9.761388
1.13851	5.965293	1.621196	10.30369
1.180483	6.507592	1.736621	10.84599
1.227702	7.049892	1.915005	11.38829
1.274921	7.592191	2.098636	11.58351
1.332634	8.13449	2.098636	11.58351
1.390346	8.67679		

CURRICULUM VITAE

Name Surname **: Muhammed Said ERGÜL**

Place and Date of Birth **: ADANA 12.09.1993**

E-Mail **: ergul16@itu.edu.tr**

EDUCATION

- **B.Sc.** **:** 2015, Iskenderun Technical University, Faculty of Engineering, Petroleum and Natural Gas Engineering

PROFESSIONAL EXPERIENCE AND REWARDS:

- 2016-Present, Research Assistant, Petroleum and Natural Gas Engineering Department, Istanbul Technical University